

2013

Assessment of detection and characterization of simulated lung nodules with low-dose CT

Kendrick J. Williams

Louisiana State University and Agricultural and Mechanical College

Follow this and additional works at: https://digitalcommons.lsu.edu/gradschool_theses



Part of the [Physical Sciences and Mathematics Commons](#)

Recommended Citation

Williams, Kendrick J., "Assessment of detection and characterization of simulated lung nodules with low-dose CT" (2013). *LSU Master's Theses*. 3320.

https://digitalcommons.lsu.edu/gradschool_theses/3320

This Thesis is brought to you for free and open access by the Graduate School at LSU Digital Commons. It has been accepted for inclusion in LSU Master's Theses by an authorized graduate school editor of LSU Digital Commons. For more information, please contact gradetd@lsu.edu.

ASSESSMENT OF DETECTION AND CHARACTERIZATION
OF SIMULATED LUNG NODULES
WITH LOW-DOSE CT

A Thesis

Submitted to the Graduate Faculty of the
Louisiana State University and
Agricultural and Mechanical College
in partial fulfillment of the
requirements for the degree of
Master of Science

in

The Department of Physics and Astronomy

by
Kendrick J. Williams
B.S., Xavier University of Louisiana, 2010
December 2013

ACKNOWLEDGMENT

First, I thank God for blessing me with this wonderful opportunity. I thank all of the members of my advisory committee: First, Dr. Matthews for serving as my advisor and mentor throughout my research experience. My appreciation is also extended to the rest of my committee: Dr. Gibbons, Dr. Hynes, Dr. Shikhaliev, and Dr. Bujenovic. I also thank all of the physicians that participated in my project: Dr. Bujenovic, Dr. Smith, Dr. Gazmen, and Dr. Gallegos. I thank my wife Jillana for all she has done in support of me during my time in graduate school. Lastly, I thank my family and friends for support and encouragement during this work.

TABLE OF CONTENTS

ACKNOWLEDGMENT.....	ii
LIST OF TABLES.....	v
LIST OF FIGURES	vi
ABSTRACT.....	vii
CHAPTER 1: INTRODUCTION.....	1
1.1 Lung Cancer.....	1
1.2 Radiological Imaging for Diagnosis of Lung Cancer.....	3
1.3 Screening for Lung Cancer.....	3
1.4 Current Recommendations for Lung Cancer Screening with CT.....	4
1.5 Review of CT Imaging.....	6
1.5.1 CT Imaging.....	6
1.5.2 Computed Tomography Dose Index.....	7
CHAPTER 2: HYPOTHESIS.....	10
2.1 Hypothesis.....	10
2.2 Specific Aims.....	10
CHAPTER 3: METHODS AND MATERIALS	13
3.1 AIM 1: Compile Database of Lung Scans with Various Acquisition Parameters and Nodule Sizes.....	13
3.1.1 CT Scanners.....	13
3.1.2 Acquisition Parameters.....	13
3.1.3 Phantom	14
3.1.4 Final Image Data Sets.....	16
3.2 AIM 2: Assessment of Image Data by Physicians.....	16
3.2.1 Displaying Image Data Sets.....	17
3.2.2 Image Assessment.....	18
3.2.3 Physician's Assessment	19
3.3 AIM 3: Compare Assessment to Known Object.....	19
3.3.1 Analysis of Sphere Size and Shape.....	19
3.3.2 Recommendation for Screening.....	20
3.4 AIM 4: Verify reliability of CTDI estimated by CT Scanner.....	20
CHAPTER 4: RESULTS AND DISCUSSION.....	22
4.1 Individual Physician's Results.....	22
4.2 4 mm Sphere Results	29
4.2.1 4 mm 80 kV Sphere Results.....	29
4.2.2 4 mm 120 kV Sphere Results.....	31
4.3 6.4 mm Sphere Results	34
4.3.1 6.4 mm 80 kV Sphere Results.....	34
4.3.2 6.4 mm 120 kV Sphere Results.....	35

4.4	8 mm Sphere Results	38
4.4.1	8 mm 80 kV Sphere Results.....	38
4.4.2	8 mm 120 kV Sphere Results.....	40
4.5	Summary of Sphere Results.....	43
4.6	CTDI Results	43
CHAPTER 5: CONCLUSION		46
REFERENCES		48
APPENDIX: PHYSICIAN INSTRUCTIONS		50
VITA.....		53

LIST OF TABLES

Table 1: Comparison of single-slice to multislice acquisition protocols(Aberle 2001)	5
Table 2: Fleischner Society Guidelines for high risk patients(MacMahon 2005)	5
Table 3: Characteristics of the CT Scanners.....	13
Table 4: Scanning Parameters.....	14
Table 5: Sizes and materials of plastic beads available to simulate lung nodules	15
Table 6: 4 mm 80 kV Sphere Results. Only acceptable images were judged for roundness and measured for sizes.	31
Table 7: 4 mm 120 kV Sphere Results. Only acceptable images were judged for roundness and measured for sizes.	33
Table 8: 6.4 mm 80 kV Sphere Results. Only acceptable images were judged for roundness and measured for sizes.	35
Table 9: 6.4 mm 120 kV Sphere Results. Only acceptable images were judged for roundness and measured for sizes.	38
Table 10: 8 mm 80 kV Sphere Results. Only acceptable images were judged for roundness and measured for sizes.	40
Table 11: 8 mm 120 kV Sphere Results. Only acceptable images were judged for roundness and measured for sizes.	42
Table 12: CTDI Comparison: Organized by Scanner and Acquisition Parameters.....	45

LIST OF FIGURES

Figure 1: Cancer deaths in 2008 in the U.S. for top 10 cancer sites (U.S. Cancer Statistics Working Group)	2
Figure 2: Concept for CT Imaging.....	7
Figure 3: Cylindrical CTDI phantom showing five holes for ion chamber placement	9
Figure 4: Photo of Anthropomorphic Torso Phantom, showing lung compartments filled with Styrofoam beads	15
Figure 5: Spheres imaged in air (left) and water (right)	16
Figure 6: Screen shot of assessment software. Three slices are shown. The tools for panning and zooming, window and leveling, and measuring image features are shown.	17
Figure 7: the three slices viewed by physicians are shown.	18
Figure 8: Plot of measured sphere size vs. physician and tube current, 4 mm sphere acquired at 80 kV and pitch > 1	23
Figure 9: Plot of measured sphere size vs. physician and tube current, 4 mm sphere acquired at 120 kV and pitch < 1	23
Figure 10: Plot of measured sphere size vs. physician and tube current, 4 mm sphere acquired at 120 kV and pitch > 1	24
Figure 11: Plot of measured sphere size vs. physician and tube current, 6.4 mm sphere acquired at 80 kV and pitch > 1	25
Figure 12: Plot of measured sphere size vs. physician and tube current, 6.4 mm sphere acquired at 120 kV and pitch < 1	26
Figure 13: Plot of measured sphere size vs. physician and tube current, 6.4 mm sphere acquired at 120 kV and pitch > 1	27
Figure 14: Plot of measured sphere size vs. physician and tube current, 8 mm sphere acquired at 80 kV and pitch > 1	28
Figure 15: Plot of measured sphere size vs. physician and tube current, 8 mm sphere acquired at 120 kV and pitch < 1	28
Figure 16: Plot of measured sphere size vs. physician and tube current, 8 mm sphere acquired at 120 kV and pitch > 1	29

ABSTRACT

Purpose: The quality of a computed tomography (CT) image and the dose delivered depend upon the acquisition parameters used to acquire the CT scan. Current, voltage and pitch are acquisition parameters that affect the image quality. The purpose of this study was to determine the influence of current, voltage and pitch on physicians' ability to characterize small, solid nodules with low-dose computed tomography.

Methods: A database of lung scans with various acquisition parameters was compiled. A torso phantom and acrylic beads were used to simulate the lungs and nodules within the lungs. Several sizes of acrylic sphere were used to simulate different size nodules. An image visualization software was used to display the images for physicians and to assess. The physicians' assessments were compared to known objects. The reliability of CTDI estimates reported by the CT acquisition software was verified.

Results: The diameter that physician's measured for the sphere became closer to the actual diameter of the sphere as the sphere size, tube current, and kVp increased. The pitch did not affect the physicians' measurement of sphere size for the larger sphere as much as it did for the smaller spheres.

Conclusion: We concluded that physicians are still able to judge size and shape of nodules accurately using low-dose CT. The 80 kV tube voltage proved to be an ineffective voltage for screening for lung cancer. Between the machines used there was not a substantial difference in perceived image quality when a current of 50 mA or higher was used. Based on this work, a low-dose protocol of 120 kV, 50 mA, and a pitch of 1.4 is recommended to balance patient dose and acceptable image quality.

CHAPTER 1: INTRODUCTION

The purpose of this study was to determine the influence of current, voltage, and pitch on the appearance of small, solid nodules with low-dose computed tomography (CT). The assessment was based on physicians' characterization of size and shape of the lung nodules. The overall image quality of a CT scan and the dose delivered is dependent upon the current, voltage and pitch used to conduct the CT scan. The quality of the image as well as the size of a lung nodule determines the physicians' ability to correctly interpret the appearance of lung nodules.

In this study, several CT datasets were taken using various imaging parameters and nodule sizes. Several physicians judged the datasets based on the images' acceptability as a screening image, distortion of the simulated lung nodule, measured nodule size, and physicians' recommended course of action.

1.1 Lung Cancer

Approximately 110,000 men and 96,000 women were diagnosed with lung cancer in 2009 in the United States. Approximately 88,000 men and 70,000 women died of lung cancer in the same year (U.S. Cancer Statistics Working Group). Although lung cancer is the second most diagnosed cancer for both men and women, it is the number one cause of cancer death (Aberle 2001, Bach 2012), as shown in **Figure 1**. The 5-year survival rate for this disease is ~15% (Aberle 2001, Bach 2012).

Top 10 Cancer Sites: 2008, Male and Female, United States—All Races

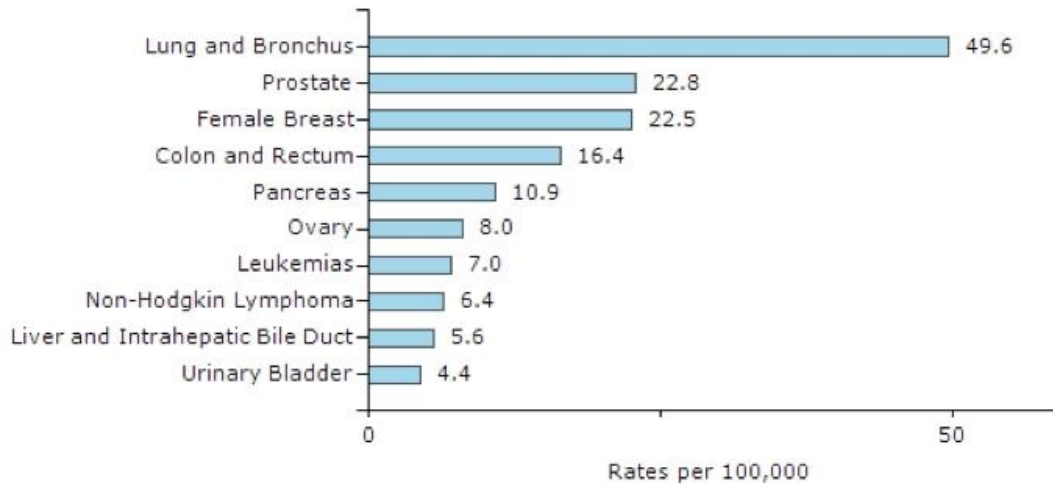


Figure 1: Cancer deaths in 2008 in the U.S. for top 10 cancer sites (U.S. Cancer Statistics Working Group)

Lung cancer is divided into two main types: small cell lung cancer (SCLC) and nonsmall cell lung cancer (NSCLC). About 25% of lung cancers are SCLC and it is widespread when it presents; the remaining 75% of lung cancers are NSCLC (Aberle 2001). Of the NSCLC, 50% to 60% present as parenchymal nodules or masses, while 40% to 50% present as central endobronchial, hilar, or mediastinal masses (Aberle 2001). Distant metastases will be present in 50% of NSCLC and only 20-25% will be potentially resectable for cure (Aberle 2001). A late stage of the disease at diagnosis is heavily related to a poor outcome (Mazzone 2012, Taiwo 2012). By controlling two pivotal factors, stage and treatment, lung cancer survival may be strongly improved (Heuvers 2012). Screening for lung cancer may reduce the risk of death from lung cancer, by allowing diagnosis at an earlier stage. Because lung cancer is often diagnosed at later stages, chemotherapy does not significantly improve the overall survival of lung cancer (Heuvers 2012). Less than 30% of cases respond to platinum based chemotherapy, which is used as a first line treatment at this stage of the disease (Heuvers 2012).

1.2 Radiological Imaging for Diagnosis of Lung Cancer

Radiological imaging is a preferred method for diagnosing lung cancer because of its noninvasive nature. Presentation with symptoms is the most common reason for performing a radiological exam to diagnose lung cancer. The typical symptoms of lung cancer, such as coughing or chest pain, may not present themselves until the disease is at a later stage (Taiwo 2012).

Chest x-rays and CT scans are the two imaging exams where lung cancer is most often detected (Taiwo 2012). Prior to the use of CT scanners, chest x-rays were the most widely used imaging exam to detect lung cancer. Initially, any nodule found on a CT scan was considered potentially malignant until it had been monitored for 2 years and found to have no growth (Revel 2004). This strategy occurred because a large portion of the nodules detected by chest radiographs were malignant but these nodules were all larger than 5 mm in diameter; most were actually 1-3 cm (Revel 2004). Several slow growing adenocarcinomas can be visualized on CT scans that were not usually visible on chest radiographs (Hasegawa 2000). CT can detect lung nodules as small as 1-2 mm in diameter (Revel 2004). Section 1.4 discusses current recommendations for lung nodule classification and follow-up.

1.3 Screening for Lung Cancer

Initially chest radiographs were evaluated for lung cancer screening. Chest radiographs did not prove to be an effective screening tool because mortality rates were not reduced (Mazzone 2012). Several studies have reported that screening for lung cancer with low-dose CT scans may help significantly reduce the mortality rate in high-risk

patients (Bach 2012, Heuvers 2012). High-risk patients are defined as those ages 55-74 with a smoking history of 30 pack-years.

Although screening for lung cancer may help people at high risk of developing lung cancer, there is a potential for harm in conducting screening (Bach 2012). Screening for lung cancer exposes an already high-risk group of individuals to radiation; radiation itself carries a risk to induce cancer. Radiation typically multiplies the background cancer risk, which is already high (Brenner 2004). Radiation-induced cancers often decrease in likelihood with increasing age at exposure; however, this pattern does not exist for radiation induced lung cancer (Brenner 2004). Risks of screening for lung cancer are discussed in more depth in Radiation Risks Potentially Associated with Low Dose CT Screening of Adult Smokers for Lung Cancer. To minimize the added risk from radiation, screening should be conducted so that as low of a dose as possible is delivered to the patient that still produces a usable image for interpretation.

1.4 Current Recommendations for Lung Cancer Screening with CT

Various groups have made contributions to the recommendations for screening for lung cancer. Annual screening, with low dose Cutoff high-risk patients for lung cancer is recommended (Aberle 2001, Hasegawa 2000). Nodules found on a CT scan are followed at intervals depending on size, growth, and calcification. Follow up of nodules detected in CT scans is recommended because some nodules will turn out to be cancers and early intervention will increase the likelihood of effective treatment (MacMahon 2005). However, large nodules are more suspicious than small nodules. Very small (<5 mm) nodules found by CT scan have a very low chance of displaying malignant behavior in a patient without a history of cancer (Henschke 2004, MacMahon 2005). Even nodules of a

slightly larger size (5-9mm) don't display malignancy in a large portion of cases (Henschke 2004).

Multirow detector CT is recommended to obtain high resolution imaging without excessive radiation. The entire thorax should be scanned in a single breath hold, if possible. Helical (spiral) scanning mode is recommended to facilitate rapid acquisition (Aberle 2001). Two example protocols are shown in **Table 1** for single-slice vs. multislice scanners.

Table 1: Comparison of single-slice to multislice acquisition protocols(Aberle 2001)

Multislice Protocol	Single Slice Spiral Scanner Protocol
○ Table feed: 30 mm per second	○ Helical mode, 0.8 seconds scan time (the shortest possible)
○ 120-140 kVp	○ 120 kVp
○ 20 to 60 mA	○ 80 mA

The Fleischner Society issued guidelines for the follow up and management of nodules found in the lung during a CT scan (MacMahon 2005). They recommended monitoring any nodule found in the lung of a high-risk patient within 12 months, with larger nodules followed up sooner. The guidelines for follow-up and management of lung nodules in high-risk patients are summarized in **Table 2**.

Table 2: Fleischner Society Guidelines for high risk patients(MacMahon 2005)

Nodule Size (mm)	Recommendation
4	Follow-up CT at 12 mo.; if unchanged, no further follow-up
>4-6	Initial follow-up CT at 6-12 mo. then at 18-24 mo. if no change
>6-8	Initial follow-up CT at 3-6 mo. then at 9-12 and 24 mo. if no change
>8	Follow-up CT at around 3, 9, and 24 mo., dynamic contrast-enhanced CT, PET, and/or biopsy

1.5 Review of CT Imaging

CT is one of the most widely used imaging modalities. By combining x-ray transmission measurements for many paths through the body, a map of the body tissues is produced. CT uses ionizing radiation, resulting in some dose to the patient. CTDI is used as a surrogate for patient dose.

1.5.1 CT Imaging

Rotating an x-ray tube around the body passes x-rays through at a large number of directions. Opposite the x-ray tube is an array of detectors to collect the transmission data. A single transmission measurement through the patient made by a single detector is called a ray. All of the rays passing through a patient at the same orientation of the x-ray tube and detector are called a projection.

Modern CT scanners use the fan beam geometry, where the rays diverge to form a fan like structure. To create the CT image from the multiple projections, a CT reconstruction algorithm is used. The most commonly used algorithm is based on filtered back projection reconstruction. This method involves smearing the attenuation data along the corresponding path in the image of the patient. The data is back projected into the image matrix, resolving correlations in measured attenuation to build up the image in the computer. **Figure 2** contains a concept drawing of CT imaging.

When referring to CT imaging, several parameters must be discussed. First, the way the CT image will be taken must be discussed. There are two acquisition modes available when taking a CT scan, helical and axial. Axial scanning involves taking static measurements. An image slice is acquired at a certain table position and then the table moves to the next position a scan will be acquired from. Helical scanning involves taking

measurements while the table the patient is laying on is moving causing the x-ray tube to move in a helical pattern around the patient. In helical scanning, a pitch must be set. The pitch describes the speed of the table motion relative to the movement of the x-ray source. The tube current influences the number of photons used to produce the CT image. The tube voltage refers to the potential difference between the anode and cathode used to create the photons. The tube voltage determines the energy spectrum of the x-ray tube. A more detailed explanation of CT imaging is provided in “The Essential Physics of Medical Imaging”.

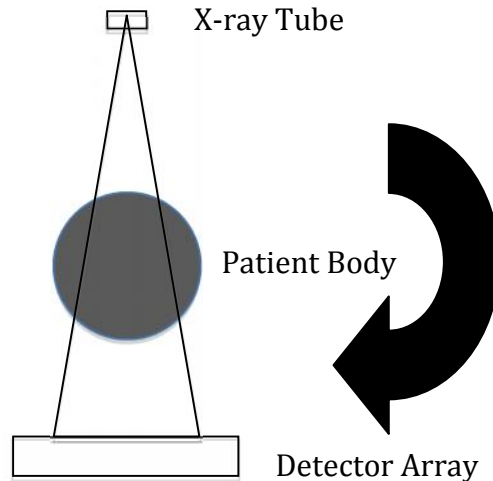


Figure 2: Concept for CT Imaging

1.5.2 Computed Tomography Dose Index

CTDI is a dose measurement concept in CT, although CTDI is not the same as patient dose (McCullough 2008). CTDI differs from patient dose in part because it is measured in a uniform cylindrical phantom. CTDI also differs from patient dose in that it is an integral dose along a line parallel to the scanner axis, rather than a point-by-point dose throughout the patient’s body or even a whole body dose. **Figure 3** illustrates the features of the cylindrical phantom used to measure CTDI. The issue with trying to

measure patient dose is that there would be different geometries for every single patient. Dose at any point in the patient is a complicated synthesis of attenuation and scatter of the x-ray beams as they travel along all possible paths to reach the point of interest. Dose measurements at points in the patient are usually impractical, as are Monte Carlo simulations of each patient.

CTDI is defined as the average absorbed dose, along the z-axis, from a series of contiguous irradiations. A single axial CT scan (one rotation of the x-ray tube) is used to measure the CTDI. It is calculated by dividing the integrated absorbed dose by the nominal total beam collimation. The CTDI is always measured in the axial scan mode for a single rotation of the x-ray source, and theoretically estimates the average dose, called the multiple scan average dose (MSAD), within the central region of a scan volume consisting of multiple, contiguous CT scans for the case where the scan length is sufficient for the central dose to approach its asymptotic upper limit (McCullough 2008). The MSAD is the average dose over an interval about the center of the scan length for a scan interval but requires multiple exposures for its direct measurement. CTDI offers a more convenient yet nominally equivalent method for estimating this. $CTDI_{100}$ is the accumulated multiple scan dose at the center of a 100 mm measurement length (McCullough 2008). The $CTDI_{100}$ is the equivalent of taking the CTDI measurement with a pencil chamber with an active length of 100 mm. The CTDI is not homogeneous throughout the field of view (FOV). The CTDI is typically a factor of two greater at the outskirts of the FOV compared to the center (McCullough 2008). Weighted CTDI ($CTDI_w$) estimates the average CTDI across the FOV. Chapter 3 explains the method for calculating $CTDI_{100}$ and $CTDI_w$ from ion chamber measurements.



Figure 3: Cylindrical CTDI phantom showing five holes for ion chamber placement

CHAPTER 2: HYPOTHESIS

2.1 Hypothesis

Computed tomography is used commonly as an imaging modality to diagnose several types of cancer including lung cancer. When scanning with CT, radiation dose is delivered to a patient; with multiple CT scans for lung cancer screening, the dose adds up from each scan. A person's risk of developing a secondary cancer increases with the total dose received. According to the linear-no threshold model any amount of radiation increases the risk of developing a radiation-induced cancer. Thus the benefit of screening for lung cancer must be weighed against the likelihood of developing a radiation-induced cancer. Lowering the dose delivered by CT during scanning for lung cancer is beneficial to the patient. Lowering dose may degrade the image quality, however, making it more difficult for physicians to accurately diagnose lung cancer. The primary thesis for this project is how does dose-level in lung CT images affect physicians' ability to correctly determine nodule shape and size. We hypothesize that only dose level and not acquisition parameters (kV, mA and pitch) will affect a physicians' ability to judge size and shape of a lung nodule in low dose CT. Specifically, any combination of kV, mA and pitch that result in comparable CTDI values will result in similar acceptable image quality. Nodule size will not influence the physicians' assessment.

2.2 Specific Aims

This thesis comprises four specific aims. The first aim compiles a database of lung scans with various acquisition parameters and lung nodule sizes. The second aim assesses the image data by physicians. The third aim compares the assessments to the known

objects in the images. The fourth aim verifies the reliability of the CTDI reported by the CT scanner.

1. Compile database of lung scans with various acquisition parameters and lung nodule sizes:

A group of images with varying doses was needed. Some image acquisition parameters affect the dose delivered by a scan, providing the means to vary dose. Combinations of parameters were selected to give a Computed Tomography Dose Index (CTDI) lower than 1.5 mGy, while dose in regular CT imaging of torso is 10 mGy. CTDI is explained in section 1.5.2. The parameters that were varied were kVp, mA, rotation speed, slice thickness, and pitch. In addition, several CT scanners were used to address the influence of different vendors and scanner designs.

A torso phantom was used to simulate the human lungs. Small plastic spheres were used to simulate lung nodules. Several materials of varying diameters were used to represent different sizes of nodules.

2. Assessment of image data by physicians:

A software interface was developed to present the images to physicians. The image database was reviewed by several physicians to assess the diagnostic quality of the images. The physicians judged the image based on several parameters such as presence, apparent size and shape, average CT number, and location of the simulated nodules.

3. Compare assessment to the known objects:

The physicians' assessment was compared to the known objects. The average sphere sizes that the physicians measured were compared to the actual sphere sizes. The spheres were classified as round or distorted by the physicians.

4. Verify reliability of CTDI estimated by CT scanner:

CT scanner acquisition software reports a CTDI dose estimated from the acquisition parameters. Although this is the dose in a predefined phantom geometry rather than the actual dose to the patient, changes in CTDI with acquisition parameters should reflect similar changes in patient dose. If this dose estimate is inaccurate, the patient may be receiving a higher than expected dose or some potential for satisfactory diagnostic quality at a lower dose may be available. Checking the accuracy of the CTDI dose will help to better select the acquisition parameters to get the best quality image at an acceptable level of dose.

CHAPTER 3: METHODS AND MATERIALS

3.1 AIM 1: Compile Database of Lung Scans with Various Acquisition Parameters and Nodule Sizes

In this section, the compilation of lung scans with various acquisition parameters is documented. These scans will be used by physicians for assessment in AIM 2.

3.1.1 CT Scanners

Three scanners were used to create the database of lung scans. Two CT scanners were located at Our Lady of the Lake Regional Medical Center (OLOL) in Baton Rouge and one CT scanner was at Mary Bird Perkins Cancer Center (MBPCC). The scanners were the GE Medical Systems Lightspeed RT16 located at MBPCC, the Siemens SOMATOM Sensation 16 located at OLOL, and the Siemens SOMATOM Sensation 64 located at OLOL. **Table 3** compares the three scanners. These scanners all had several different reconstruction algorithms. The algorithm specified for lung scans was used with each of the CT scanners. Helical image data was acquired from each scanner.

Table 3: Characteristics of the CT Scanners

	Lightspeed RT16	Sensation 16	Sensation 64
Detector size	0.625 mm	0.75 mm	0.6 mm
# of Detector rows	16	16	64
Tube Voltage	80-140 kV*	80-140 kV*	80-140 kV*
Scan FOV	50 cm	50 cm	50 cm
Rotation Times	0.8, 0.9, 1.0 s	0.42, 0.5, 0.75, 1, 1.5 s	0.5, 1, 1.5 s
Table speeds (or pitches)	.938, 1.375	1-150 mm/s [^]	0.45-2.0 [^]
Manufacturer	GE	Siemens	Siemens

* Discrete interval only ^ Continuous spectrum

3.1.2 Acquisition Parameters

Several acquisition parameters were varied for this study. Each CT scanner had a different set of parameter values, so the parameters between each scanner were matched as closely as possible. **Table 4** summarizes the parameters used. Similar rotation times

were used for the Lightspeed RT16 and Sensation 16, while a shorter rotation time was used for the Sensation 64. The pitch and table speed of the Lightspeed RT16 was used as the target value for the other two machines. The Sensation 16 was set for similar table speed. The Sensation 64 was set for similar pitch.

Table 4: Scanning Parameters

	Lightspeed RT16		Sensation 16		Sensation 64	
kVp (kV)	80	120	80	120	80	120
Current (mA)	50,100	35,50	50,100	35,50	50,100	35,50
Rotation Time (s)	0.8		0.75		0.5	
Pitch	1.4	0.94,1.4	--	--	1.4	0.95, 1.4
Table Speed	27.5	18.75, 27.5	28	18.1, 28	--	--

3.1.3 Phantom

The phantom used in this experiment was made of two parts, a torso phantom and plastic spheres. The anthropomorphic torso phantom was used to simulate the human lung and the body around it. The torso phantom is shown in **Figure 4**. The torso phantom included two lung compartments filled with water and Styrofoam beads to simulate the attenuation of the human lung. Because the phantom was originally designed for assessing nuclear cardiac imaging, only the base of the lungs were represented. A Teflon rod simulated the spine's attenuating ability. The liver and background compartments were filled with water. The phantom's cardiac insert was not used for imaging.

Several types and sizes of spheres were used to simulate lung nodules of varying densities and sizes. Five materials and 6 sizes were considered, shown in **Table 5**. These materials exhibited a range of densities; some of the materials were less dense than water and some of the materials were denser than water. **Figure 5** shows an image of all the spheres imaged in air and in water. The spheres imaged in air were taped to a Styrofoam block. The spheres imaged in water were glued to a block of solid water and placed

inside a tub of water. The spheres in air and in water were imaged at diagnostic quality, at a tube current between 150 mA – 440 mA. A kVp of 80 kV, 100 kV, 120 kV and 140 kV was used. A reconstructed slice width between 1.25 mm, 2.50 mm and 5 mm was used. These images show how the spheres appear on a diagnostic quality image; if a sphere is not visible on a diagnostic image then it will not be visible on a screening image. These images were used to determine which parameters to use to create the image database.

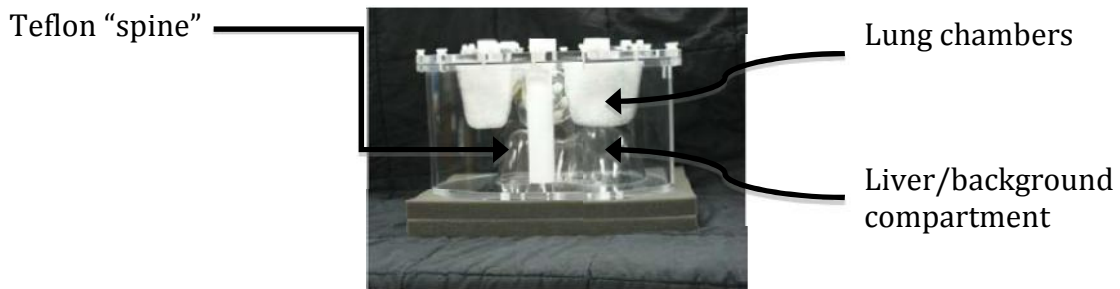


Figure 4: Photo of Anthropomorphic Torso Phantom, showing lung compartments filled with Styrofoam beads

Table 5: Sizes and materials of plastic beads available to simulate lung nodules

Nominal Sizes (inch)	Nominal Sizes (mm)	Acrylic	HDPE	Nylon	Polypropylene	PTFE
1/16	1.6	X	X	X	X	X
1/8	3.2	X	X	X	X	X
5/32	4.0	X	X	X	X	X
3/16	4.8	X		X	X	X
1/4	6.4	X	X	X	X	X
5/16	7.9	X		X		X
Density (g/cm³)		1.19	0.95	1.10	0.95	2.20

X indicates the size of material combination was available for consideration

These spheres are placed within the lung chamber of the torso phantom and imaged with the various acquisition parameters. First, the liver and background compartment were filled with water. Next, the lung compartments were filled with water. Then, a different size sphere is placed in each lung at a randomly chosen depth. The phantom is placed on its back and multiple acquisitions for each pair of beads are taken without moving the phantom.

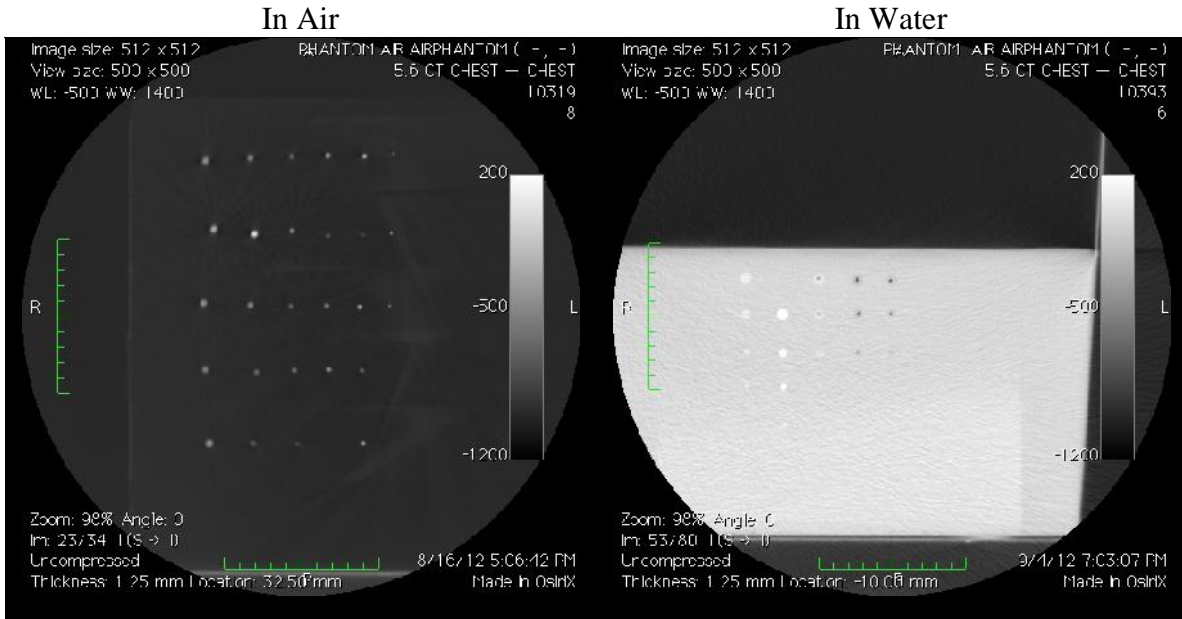


Figure 5: Spheres imaged in air (left) and water (right)

3.1.4 Final Image Data Sets

The final image data sets used by physicians contained neither all the spheres nor all possible combination of acquisition parameters. This was done to limit the number of images each physician would have to view. Only the acrylic sphere was used because it was the densest and showed the best in water. Three sizes were selected for the physician’s assessment, which were 4 mm, 6.35 mm, and 8 mm spheres. These sizes were chosen because they span the Fleischner Society’s guidelines. The final image data sets consisted of 81 sets of 3 CT slices each, including the slice with the sphere as well as the next inferior and superior slices. The physicians viewed each set of three slices lined up beside one another. All of this data was included in the quantitative assessment.

3.2 AIM 2: Assessment of Image Data by Physicians

In this section, the method for physician review of images and assessment of the diagnostic quality is described.

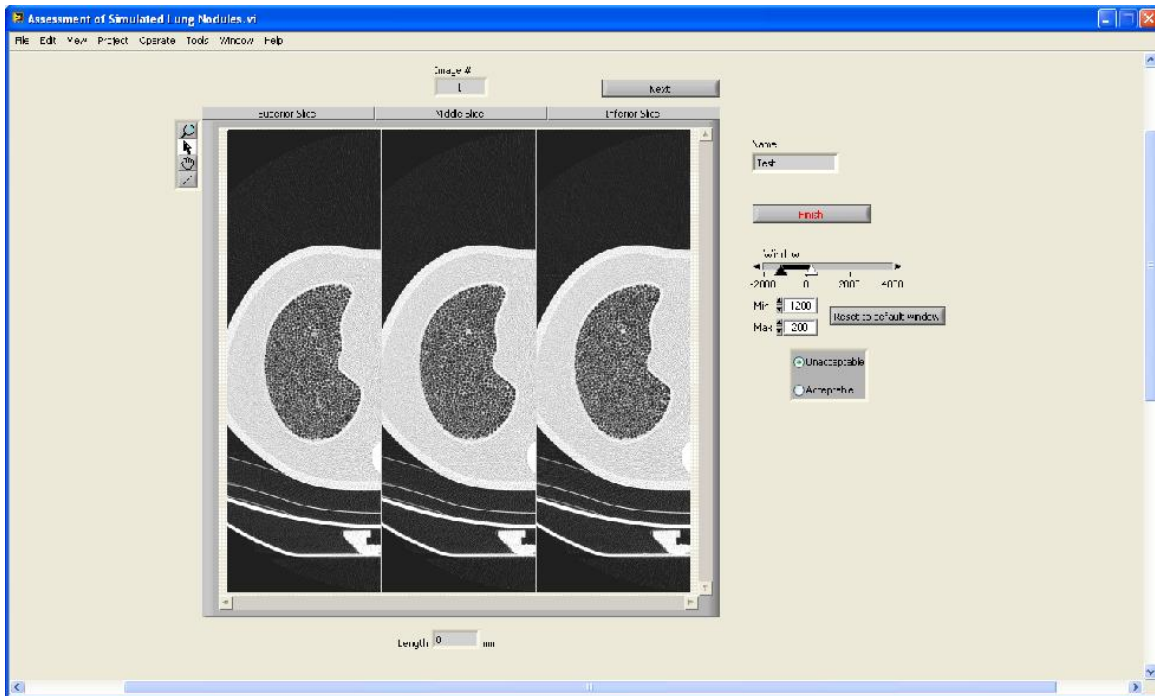


Figure 6: Screen shot of assessment software. Three slices are shown. The tools for panning and zooming, window and leveling, and measuring image features are shown.

3.2.1 Displaying Image Data Sets

The images were displayed using software created in LabVIEW (National Instruments version 8.2) and had several features. Although not as full-featured as most clinical radiology viewing stations, this software provided a consistent platform for all the physicians. **Figure 6** shows a screen shot of the software. This avoided variations in vendor platforms at different institutions, and allowed automation of response collection from the physicians. Three transverse CT slices were shown simultaneously for the observer to view. Several tools were available to manipulate the images. The instructions provided to the physicians are included in the Appendix. The software provided tools to zoom and pan the images, window and level the display, and measure image features.

3.2.2 Image Assessment

Each image set was displayed to the observer. All three slices in a set were shown side by side. An image of all three slices is shown in **Figure 7**. The observer would adjust the window and level to a suitable setting. The observer then decided whether the image quality was acceptable for a screening image. If the image was not acceptable, no further questions were asked about the image. If the image was acceptable, the observer was given a set of three questions to answer.

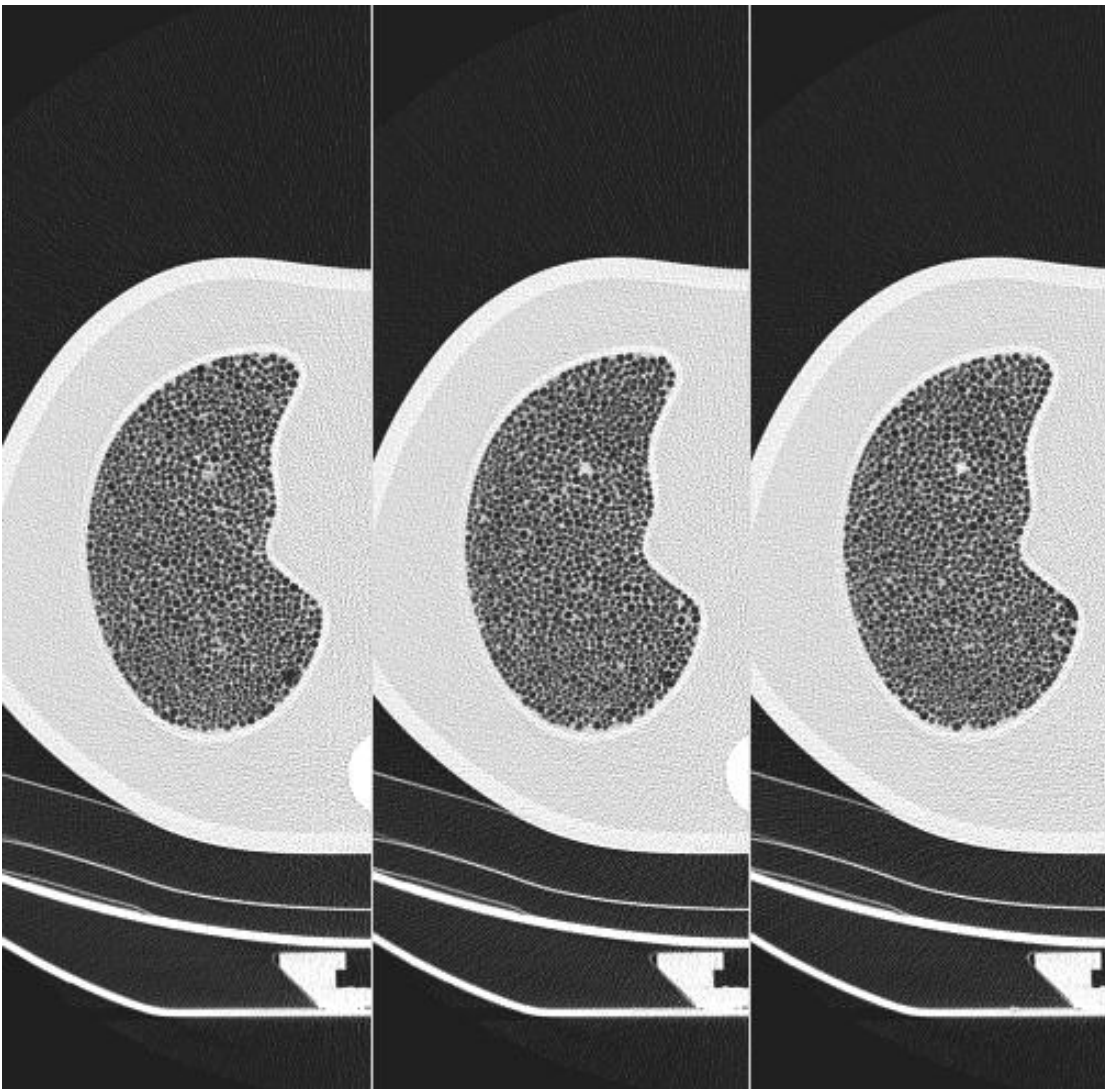


Figure 7: the three slices viewed by physicians are shown.

The observer was first asked if the nodule within the CT slice appeared round or distorted. Either way, the observer was asked to measure the length of the nodule; if the nodule was distorted, the observer was asked to measure the long axis dimension. The observer was then asked to select a recommended course of action from a list based on the guidelines established by the Fleischner Society (MacMahon 2005).

This process was repeated for all 81 images used within the study. The CT images were presented in a randomized order to each observer.

3.2.3 Physician's Assessment

The data collected from the observers were categorized by current (35, 50, or 100 mA), kilovoltage (80 or 120 kV), pitch (low or high), machine (Lightspeed RT16, Sensation 16 or Sensation 64) and sphere size (4, 6.35, 8 mm). This response data was then analyzed to determine which combination of parameters gave an acceptable image while not exceeding the recommended CTDI. These responses were also used to categorize differences between the different scanners.

3.3 AIM 3: Compare Assessment to Known Object

3.3.1 Analysis of Sphere Size and Shape

The fraction of images for each dose level rated as acceptable was determined. The fraction of images for each dose level rated as round was also determined. The diameters of the spheres as measured by the physicians were averaged and compared to the nominal diameters. Since within the scanning software, a physician is forced to click inside of a single pixel uncertainty will present within the measurements. This uncertainty was quantified as the diagonal of one pixel. Since the pixel from each scanner vary in size, the average of the three is used to determine this uncertainty.

3.3.2 Recommendation for Screening

The assessment given by the physicians was used to rate the utility of each combination of scanning parameters for screening. This was based on the number of physicians that agreed the image was acceptable, with an undistorted nodule shape and accurate measured size.

3.4 AIM 4: Verify reliability of CTDI estimated by CT Scanner

The final task of this project was to compare the dose delivered for various scanning parameters to the dose estimated by the CT scanner. The CTDI estimate provided by the CT scanner and the measured CTDI must match well, if the estimated CTDI is to be trusted as a surrogate for reducing patient dose.

The CTDI for each set of acquisition parameters was measured using the formulism discussed in AAPM Task Group Report 23 (TG 23) (McCullough 2008). A standard CTDI phantom of 32 cm diameter was used to take ionization measurements. The acrylic phantom had five holes drilled into it: at the center, top, bottom (meaning closest to the table), left, and right sides. This was shown in **Figure 3**. An ion chamber (Radcal 10X9-3CT, S/N 05-0002) and electrometer (Radcal 9095, S/N 95-0015) were used to measure exposure, which was then converted to dose. $CTDI_{100}$ was calculated from the ion chamber reading by

$$CTDI_{100}(rad) = \frac{C \cdot f(rad/R) \cdot (100 \text{ mm}) \cdot meter \text{ reading}(R)}{N \cdot T(mm)} \quad \text{Equation 1}$$

C = the unit less calibration factor, this was stored inside the electrometer

f = factor to convert exposure to absorbed dose, an f factor of 0.87 was used

N = number of tomographic sections imaged in a single axial scan

T = the width of the tomographic section along the z axis imaged by one data channel (McCullough 2008)

Three measurements were taken in the acrylic phantom at the center and the edge. The top edge was used as recommended by reference 4. $CTDI_{100}$ was calculated for each position. Weighted CTDI ($CTDI_w$) was then calculated by

$$CTDI_w = 1/3CTDI_{100,center} + 2/3CTDI_{100,edge} \quad \text{Equation 2}$$

where

$CTDI_{100, center} = CTDI_{100}$ measured at the center of the CTDI phantom

$CTDI_{100, edge} = CTDI_{100}$ measured at the top edge of the CTDI phantom

The calculated $CTDI_w$ was then compared to the $CTDI_w$ reported by the scanner software; percent difference was calculated by

$$\% \text{ diff} = \frac{CTDI_w(\text{Software}) - CTDI_w(\text{Measured})}{CTDI_w(\text{Software})} \quad \text{Equation 3}$$

and error was determined from the standard deviation of the ion chamber measurements. A positive % diff is considered good and a negative % diff is considered bad. A positive % diff means the scanner is overestimating the actual dose.

CHAPTER 4: RESULTS AND DISCUSSION

This chapter is laid out in five sections. The first section shows the individual physician's results for the different sizes of spheres. The next three sections show each physician's results for all three sizes of spheres. The fifth section gives the results from the CTDI measurements. The three sections showing physician results for the three sizes of spheres size are subdivided in two parts:

1. the results from imaging the spheres at 80 kV
2. the results from imaging the spheres at 120 kV.

4.1 Individual Physician's Results

Figures 8-16 below show all of the results at a glance. The images taken of the 4 mm sphere at 80 kV with a pitch greater than 1 are shown in **Figure 8**. Four of 12 were rated as acceptable for Sensation 16. Two of 4 were within one uncertainty of the correct sphere size for Sensation 16. Six of 12 were rated as acceptable for Sensation 64. Four of 6 were within one uncertainty of the correct sphere size for Sensation 64. Five of 12 were rated as acceptable for Lightspeed RT16. Three of 5 were within one uncertainty of the correct sphere size for Lightspeed RT16.

The images taken of the 4 mm sphere at 120 kV and a pitch less than 1 are shown in **Figure 9**. Ten of 12 were rated as acceptable for Sensation 16. Seven of 10 were within one uncertainty of the correct sphere size for Sensation 16. Ten of 12 were rated as acceptable for Sensation 64. Six of 10 were within one uncertainty of the correct sphere size for Sensation 64. Eleven of 12 were rated as acceptable for Lightspeed RT16. Three of 11 were within one uncertainty of the correct sphere size for Lightspeed RT16.

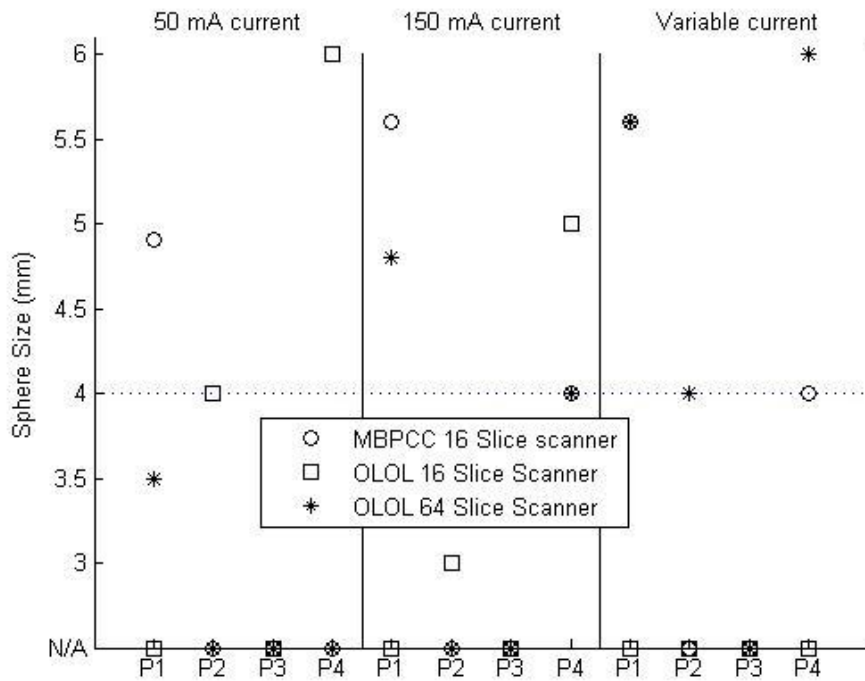


Figure 8: Plot of measured sphere size vs. physician and tube current, 4 mm sphere acquired at 80 kV and pitch > 1

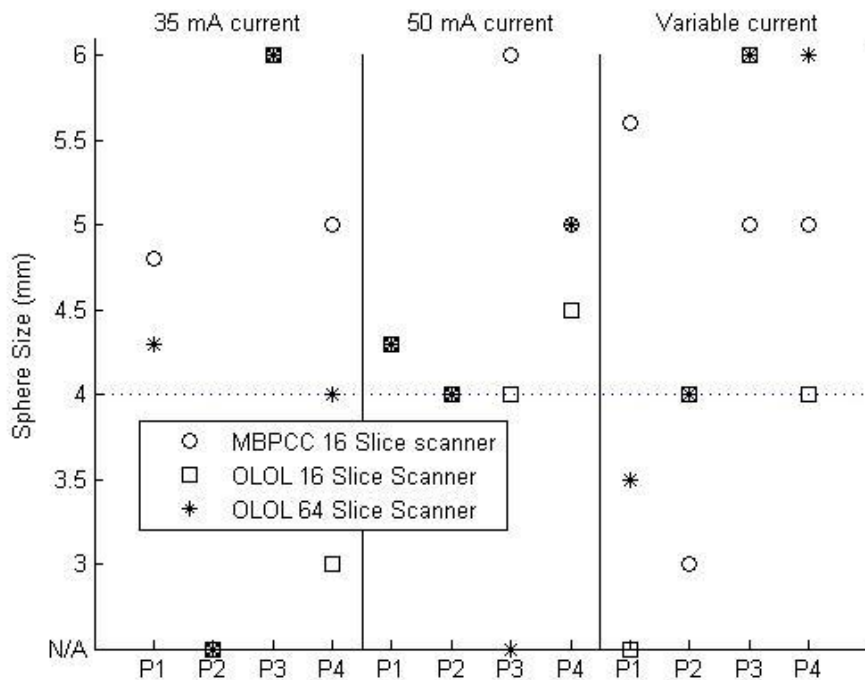


Figure 9: Plot of measured sphere size vs. physician and tube current, 4 mm sphere acquired at 120 kV and pitch < 1

The images taken of the 4 mm sphere at 120 kV and a pitch greater than 1 are shown in **Figure 10**. Eleven of 12 were rated as acceptable for Sensation 16. Seven of 11 were within one uncertainty of the correct sphere size for Sensation 16. Twelve of 12 were rated as acceptable for Sensation 64. Eleven of 12 were within one uncertainty of the correct sphere size for Sensation 64. Eleven of 12 were rated as acceptable for Lightspeed RT16. Three of 11 were within one uncertainty of the correct sphere size for Lightspeed RT16.

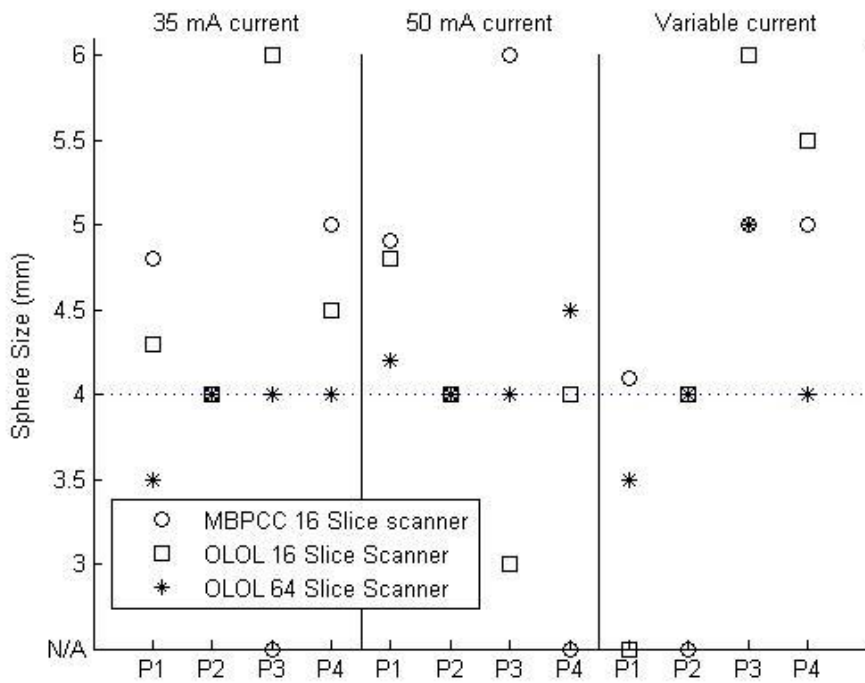


Figure 10: Plot of measured sphere size vs. physician and tube current, 4 mm sphere acquired at 120 kV and pitch > 1

The images taken of the 6.4 mm sphere at 80 kV are shown in **Figure 11**. Eleven of 12 were rated as acceptable for Sensation 16. Five of 11 were within one uncertainty of the correct sphere size for Sensation 16. Five of 12 were rated as acceptable for Sensation 64. Three of 5 were within one uncertainty of the correct sphere size for Sensation 64.

Five of 12 were rated as acceptable for Lightspeed RT16. Three of 5 were within one uncertainty of the correct sphere size for Lightspeed RT16.

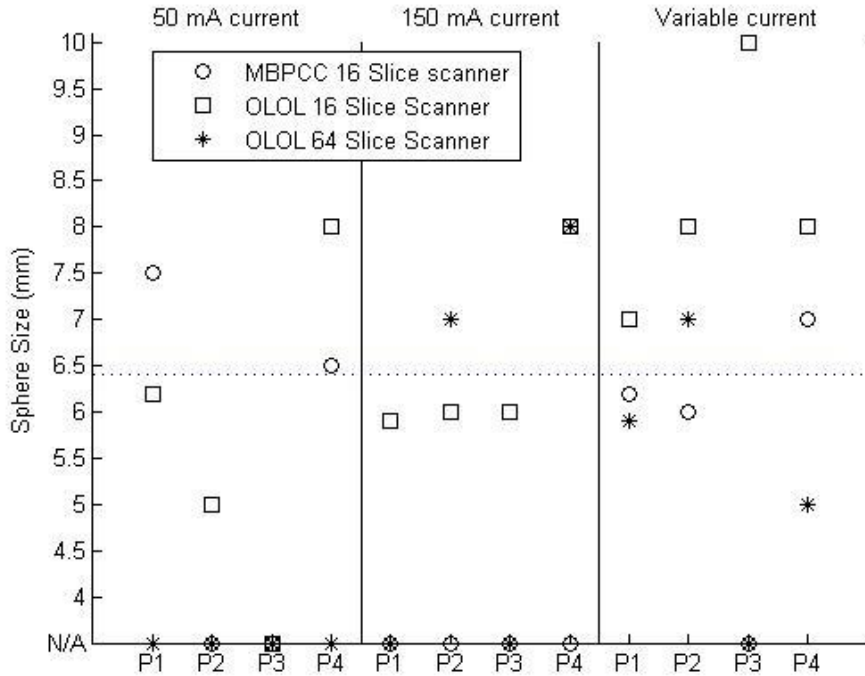


Figure 11: Plot of measured sphere size vs. physician and tube current, 6.4 mm sphere acquired at 80 kV and pitch > 1

The images taken of the 6.4 mm sphere at 120 kV and a pitch less than 1 are shown in **Figure 12**. Twelve of 12 were rated as acceptable for Sensation 16. Seven of 12 were within one uncertainty of the correct sphere size for Sensation 16. Ten of 12 were rated as acceptable for Sensation 64. Four of 10 were within one uncertainty of the correct sphere size for Sensation 64. Nine 12 were rated as acceptable for Lightspeed RT16. Six of 9 were within one uncertainty of the correct sphere size for Lightspeed RT16.

The images taken of the 6.4 mm sphere at 120 kV and a pitch greater than 1 are shown in **Figure 13**. Nine of 12 were rated as acceptable for Sensation 16. Six of 9 were within one uncertainty of the correct sphere size for Sensation 16. Eleven of 12 were rated as acceptable for Sensation 64. Five of 11 were within one uncertainty of the correct

sphere size for Sensation 64. Ten of 12 were rated as acceptable for Lightspeed RT16. Seven of 10 were within one uncertainty of the correct sphere size for Lightspeed RT16.

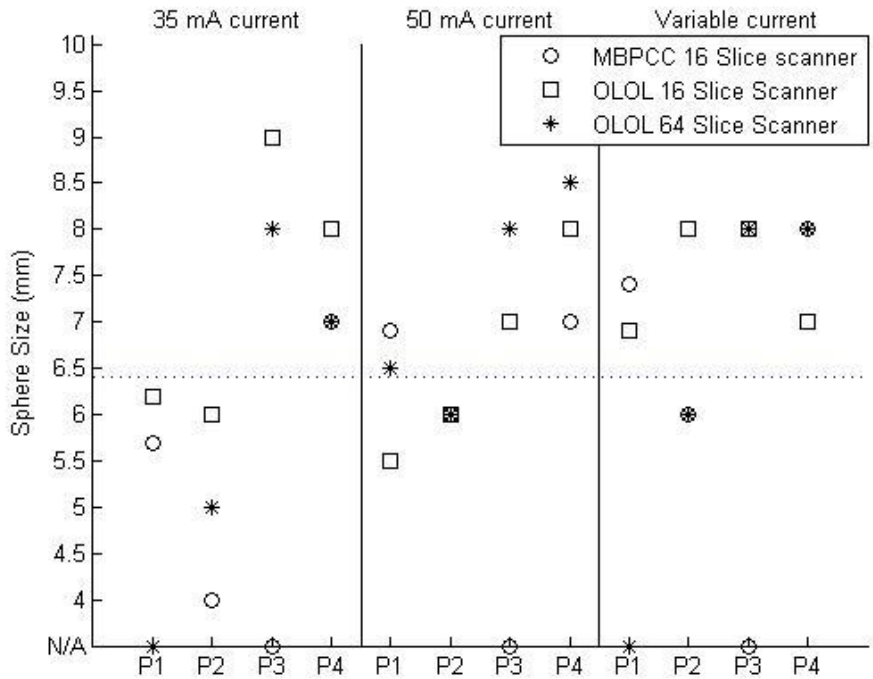


Figure 12: Plot of measured sphere size vs. physician and tube current, 6.4 mm sphere acquired at 120 kV and pitch < 1

The images taken of the 8 mm sphere at 80 kV are shown in **Figure 14**. Ten of 12 were rated as acceptable for Sensation 16. Eight of 10 were within one uncertainty of the correct sphere size for Sensation 16. Nine of 12 were rated as acceptable for Sensation 64. Seven of 9 were within one uncertainty of the correct sphere size for Sensation 64. Five of 12 were rated as acceptable for Lightspeed RT16. Four of 5 were within one uncertainty of the correct sphere size for Lightspeed RT16.

The images taken of the 8 mm sphere at 120 kV and a pitch less than 1 are shown in **Figure 15**. Twelve of 12 were rated as acceptable for Sensation 16. Nine of 12 were within one uncertainty of the correct sphere size for Sensation 16. Twelve of 12 were

rated as acceptable for Sensation 64. Five of 12 were within one uncertainty of the correct sphere size for Sensation 64. Ten of 12 were rated as acceptable for Lightspeed RT16.

Ten of 10 were within one uncertainty of the correct sphere size for Lightspeed RT16.

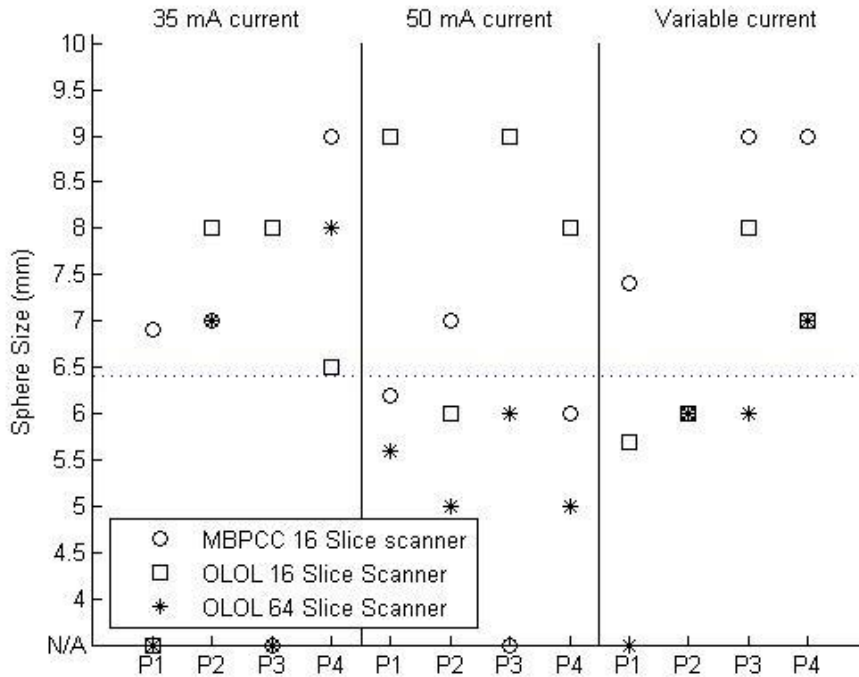


Figure 13: Plot of measured sphere size vs. physician and tube current, 6.4 mm sphere acquired at 120 kV and pitch > 1

The images taken of the 8 mm sphere at 120 kV and a pitch greater than 1 are shown in **Figure 16**. Twelve of 12 were rated as acceptable for Sensation 16. Eleven of 12 were within one uncertainty of the correct sphere size for Sensation 16. Twelve of 12 were rated as acceptable for Sensation 64. Twelve of 12 were within one uncertainty of the correct sphere size for Sensation 64. Nine of 12 were rated as acceptable for Lightspeed RT16. Eight of 9 were within one uncertainty of the correct sphere size for Lightspeed RT16.

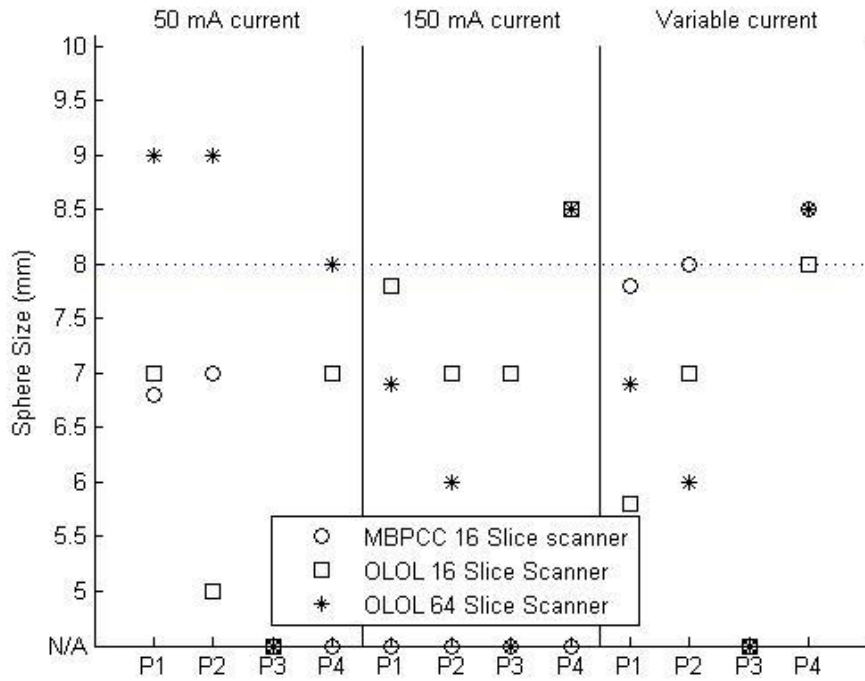


Figure 14: Plot of measured sphere size vs. physician and tube current, 8 mm sphere acquired at 80 kV and pitch > 1

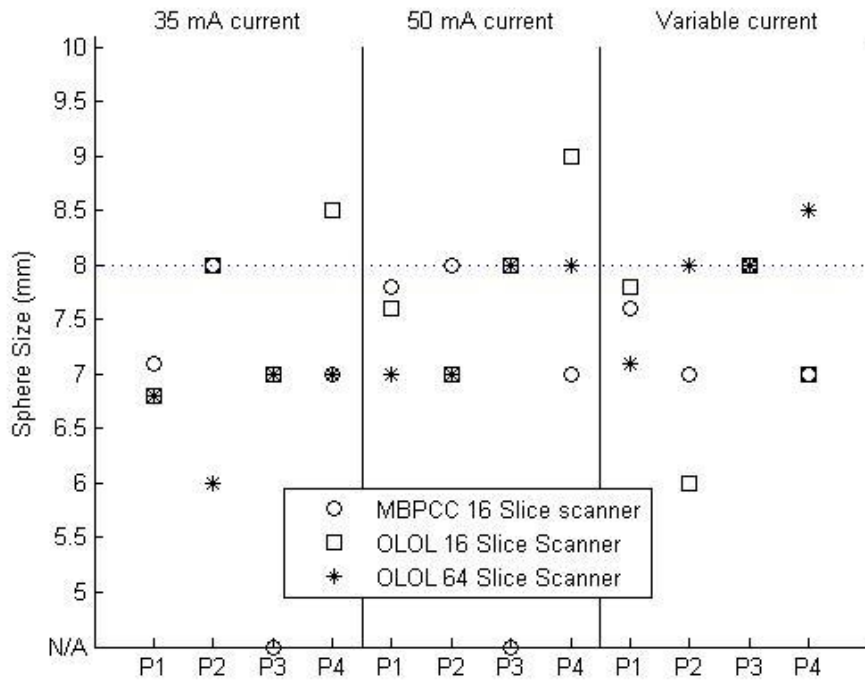


Figure 15: Plot of measured sphere size vs. physician and tube current, 8 mm sphere acquired at 120 kV and pitch < 1

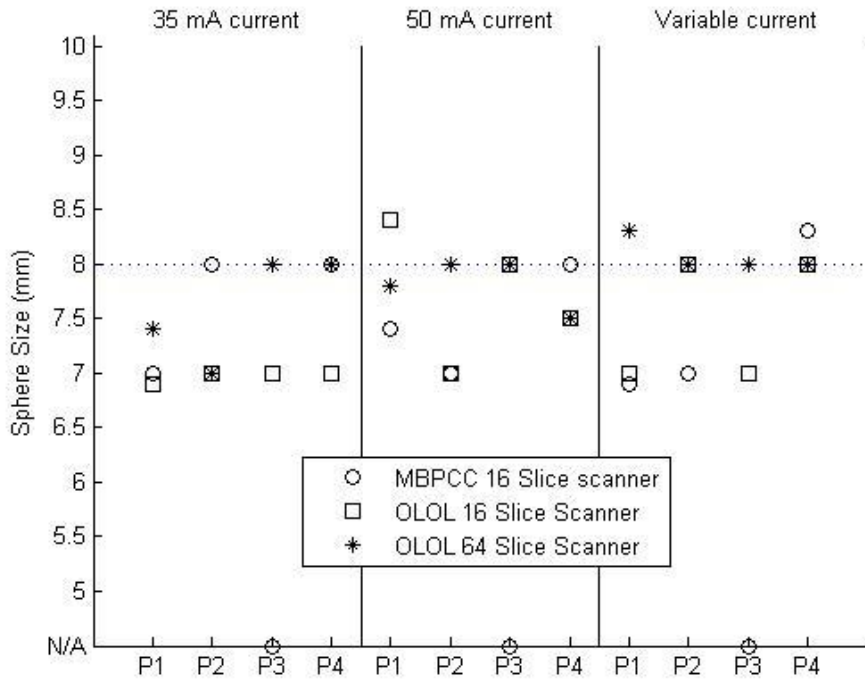


Figure 16: Plot of measured sphere size vs. physician and tube current, 8 mm sphere acquired at 120 kV and pitch > 1

4.2 4 mm Sphere Results

The results detailed in this section apply to 4 mm diameter spheres measured on the three different CT scanners, combined for all four physicians.

4.2.1 4 mm 80 kV Sphere Results

Ideally, all of the physicians will agree on which images are of acceptable or unacceptable image quality, as well as which images are round and distorted. Ideally, every image should exhibit both acceptable image quality and a round shape for the sphere. There should also be agreement between the Lightspeed RT16 and the Sensation 16. This did not actually occur. There are several variations on the physicians' responses based on the scanner and even within a single image. **Table 6** summarizes the results for 4 mm spheres at 80 kV, different mA, and different pitches.

The physicians' ratings of the image taken from all scanners at 80 kV and 50 mA were very similar. Two of the physicians rated the image as acceptable for the Sensation 16. These two physicians both agreed that the sphere within the image was round. The average measurement of the sphere was 5.00 ± 1.00 mm. The other two physicians rated the image as unacceptable. For the Sensation 64, 3 physicians rated the image as unacceptable. One physician rated the image as acceptable but not round. The average measurement for the Sensation 64 was 3.50 mm. For the Lightspeed RT16, three physicians rated the image as unacceptable. One physician rated the image as acceptable but not round. The average measurement for the Lightspeed RT16 was 4.90 mm.

The physicians' rating of the images taken from all the scanners at 80 kV and 100 mA were consistent across the three machines. Two of the physicians rated the image as acceptable for the Sensation 16. One physician rated the sphere within the image as round. The average measurement of the sphere was 4.00 ± 1.00 mm. The other two physicians rated the image as unacceptable. For the Sensation 64, two physicians rated the image as acceptable. One physician rated the sphere within the image as round. The average measurement for the Sensation 64 was 4.40 ± 0.40 mm. For the Lightspeed RT16, two physicians rated the image as acceptable. None of the physicians rated the image as round. The average measurement for the Lightspeed RT16 was 4.80 ± 0.80 mm.

The physicians' rating of the images taken from all the scanners at 80 kV and a variable current showed a variation from machine to machine. None of the physicians rated the image as acceptable for the Sensation 16. For the Sensation 64, three physicians rated the image as acceptable. One physician rated the sphere within the image as round. The average measurement for the Sensation 64 was 5.20 ± 0.86 mm. For the Lightspeed

RT16, two physicians rated the image as acceptable. One of the physicians rated the image as round. The average measurement for the Lightspeed RT16 was 5.05 ± 0.95 mm.

Table 6: 4 mm 80 kV Sphere Results. Only acceptable images were judged for roundness and measured for sizes.

Sphere	Center	kV	mA	Pitch	Average	St. Dev.	Unacceptable	Acceptable	Round
4	Sensation 16	80	50	H	5.00	1.00	2	2	2
4	Sensation 64	80	50	H	3.50	--	3	1	0
4	Lightspeed RT16	80	50	L	4.90	--	3	1	0
4	Sensation 16	80	100	H	4.00	1.00	2	2	1
4	Sensation 64	80	100	H	4.40	0.40	2	2	1
4	Lightspeed RT16	80	100	L	4.80	0.80	2	2	0
4	Sensation 16	80	Variable	H	--	--	4	0	0
4	Sensation 64	80	Variable	H	5.20	0.86	1	3	1
4	Lightspeed RT16	80	Variable	L	5.05	0.95	2	2	1

4.2.2 4 mm 120 kV Sphere Results

Table 7 summarizes the results for 4 mm spheres at 120 kV and different mA. The physicians' rating of the images taken from all the scanners at 120 kV, 35 mA, and a pitch greater than 1 showed little variation from machine to machine. None of the physicians rated the image as acceptable for the Sensation 16. For the Sensation 64, all of the physicians rated the image as acceptable. Three of the physicians rated the sphere within the image as round. The average measurement for the Sensation 64 was 3.88 ± 0.22 mm. For the Lightspeed RT16, three physicians rated the image as acceptable. None of the physicians rated the image as round. The average measurement for the Lightspeed RT16 was 4.60 ± 0.43 mm.

The physicians' rating of the images taken from all the scanners at 120 kV, 35 mA, and a pitch less than 1 showed little variation from machine to machine. Three of the physicians rated the image as acceptable for the Sensation 16. One of the physicians rated the sphere within the image as round. The average measurement of the sphere was $5.07 \pm$

1.46 mm. For the Sensation 64, three of the physicians rated the image as acceptable. Two of the physicians rated the sphere within the image as round. The average measurement for the Sensation 64 was 4.77 ± 0.88 mm. For the Lightspeed RT16, three of the physicians rated the image as acceptable. One of the physicians rated the image as round. The average measurement for the Lightspeed RT16 was 5.27 ± 0.52 mm.

The physicians' rating of the images taken from all the scanners at 120 kV, 50 mA, and a pitch greater than 1 showed little variation from machine to machine. All of the physicians rated the image as acceptable for the Sensation 16. All of the physicians rated the sphere within the image as round. The average measurement of the sphere was 3.95 ± 0.64 mm. For the Sensation 64, all of the physicians rated the image as acceptable. All of the physicians rated the sphere within the image as round. The average measurement for the Sensation 64 was 4.18 ± 0.20 mm. For the Lightspeed RT16, three of the physicians rated the image as acceptable. None of the physicians rated the image as round. The average measurement for the Lightspeed RT16 was 4.97 ± 0.82 mm.

The physicians' rating of the images taken from all the scanners at 120 kV, 50 mA, and a pitch less than 1 showed little variation from machine to machine. All of the physicians rated the image as acceptable for the Sensation 16. One of the physicians rated the sphere within the image as round. The average measurement of the sphere was 4.20 ± 0.21 mm. For the Sensation 64, three of the physicians rated the image as acceptable. Two of the physicians rated the sphere within the image as round. The average measurement for the Sensation 64 was 4.43 ± 0.42 mm. For the Lightspeed RT16, all of the physicians rated the image as acceptable. One of the physicians rated the image as round. The average measurement for the Lightspeed RT16 was 4.83 ± 0.77 mm.

The physicians' rating of the images taken from all the scanners at 120 kV, a variable current, and a pitch greater than 1 showed little variation from machine to machine. Three of the physicians rated the image as acceptable for the Sensation 16. One of the physicians rated the sphere within the image as round. The average measurement of the sphere was 5.17 ± 0.85 mm. For the Sensation 64, all of the physicians rated the image as acceptable. All of the physicians rated the sphere within the image as round. The average measurement for the Sensation 64 was 4.13 ± 0.54 mm. For the Lightspeed RT16, three of the physicians rated the image as acceptable. One of the physicians rated the image as round. The average measurement for the Lightspeed RT16 was 4.70 ± 0.42 mm.

Table 7: 4 mm 120 kV Sphere Results. Only acceptable images were judged for roundness and measured for sizes.

Sphere	Center	kV	mA	Pitch	Average	St. Dev.	Unacceptable	Acceptable	Round
4	Lightspeed RT16	120	35	H	4.60	0.43	1	3	0
4	Sensation 16	120	35	H	4.70	0.77	0	4	2
4	Sensation 64	120	35	H	3.88	0.22	0	4	3
4	Lightspeed RT16	120	35	L	5.27	0.52	1	3	1
4	Sensation 16	120	35	L	5.07	1.46	1	3	1
4	Sensation 64	120	35	L	4.77	0.88	1	3	2
4	Lightspeed RT16	120	50	H	4.97	0.82	1	3	0
4	Sensation 16	120	50	H	3.95	0.64	0	4	4
4	Sensation 64	120	50	H	4.18	0.20	0	4	4
4	Lightspeed RT16	120	50	L	4.83	0.77	0	4	1
4	Sensation 16	120	50	L	4.20	0.21	0	4	1
4	Sensation 64	120	50	L	4.43	0.42	1	3	2
4	Lightspeed RT16	120	Variable	H	4.70	0.42	1	3	1
4	Sensation 16	120	Variable	H	5.17	0.85	1	3	1
4	Sensation 64	120	Variable	H	4.13	0.54	0	4	4
4	Lightspeed RT16	120	Variable	L	4.65	0.98	0	4	0
4	Sensation 16	120	Variable	L	4.67	0.94	1	3	1
4	Sensation 64	120	Variable	L	4.88	1.14	0	4	1

The physicians' rating of the images taken from all the scanners at 120 kV, a variable current, and a pitch less than 1 showed little variation from machine to machine. Three of

the physicians rated the image as acceptable for the Sensation 16. One of the physicians rated the sphere within the image as round. The average measurement of the sphere was 4.67 ± 0.94 mm. For the Sensation 64, all of the physicians rated the image as acceptable. One of the physicians rated the sphere within the image as round. The average measurement for the Sensation 64 was 4.88 ± 1.14 mm. For the Lightspeed RT16, all of the physicians rated the image as acceptable. None of the physicians rated the image as round. The average measurement for the Lightspeed RT16 was 4.65 ± 0.98 mm.

4.3 6.4 mm Sphere Results

4.3.1 6.4 mm 80 kV Sphere Results

Table 8 summarizes the results for 4 mm spheres at 120 kV and different mA. The physicians' rating of the images taken from all scanners at 80 kV and 50 mA varied from machine to machine. Three of the physicians rated the image as acceptable for the Sensation 16. One of the physicians rated the sphere within the image as round. The average measurement of the sphere was 6.40 ± 1.23 mm. For the Sensation 64, none of the physicians rated the image as acceptable. For the Lightspeed RT16, two of the physicians rated the image as acceptable. One of the physicians rated the image as round. The average measurement for the Lightspeed RT16 was 6.95 ± 0.45 mm.

The physicians' rating of the images taken from all the scanners at 80 kV and 100 mA varied from machine to machine. All of the physicians rated the image as acceptable for the Sensation 16. None of the physicians rated the sphere within the image as round. The average measurement of the sphere was 6.48 ± 0.88 mm. For the Sensation 64, two of the physicians rated the image as acceptable. One of the physicians rated the sphere within the image as round. The average measurement for the Sensation 64 was 7.50 ± 0.50 mm.

The physicians' rating of the images taken from all scanners at 80 kV and a variable current showed little variation from machine to machine. All of the physicians rated the image as acceptable for the Sensation 16. None of the physicians rated the sphere within the image as round. The average measurement of the sphere was 8.25 ± 1.09 mm. For the Sensation 64, three of the physicians rated the image as acceptable. Two of the physicians rated the sphere within the image as round. The average measurement for the Sensation 64 was 5.97 ± 0.82 mm. For the Lightspeed RT16, three of the physicians rated the image as acceptable. Two of the physicians rated the image as round. The average measurement for the Lightspeed RT16 was 6.40 ± 0.43 mm.

Table 8: 6.4 mm 80 kV Sphere Results. Only acceptable images were judged for roundness and measured for sizes.

Sphere	Center	kV	mA	Pitch	Average	St. Dev.	Unacceptable	Acceptable	Round
6.4	Sensation 16	80	50	H	6.40	1.23	1	3	1
6.4	Sensation 64	80	50	H	--	--	4	0	0
6.4	Lightspeed RT16	80	50	L	6.95	0.45	2	2	1
6.4	Sensation 16	80	100	H	6.48	0.88	0	4	0
6.4	Sensation 64	80	100	H	7.50	0.50	2	2	1
6.4	Sensation 16	80	Variable	H	8.25	1.09	0	4	0
6.4	Sensation 64	80	Variable	H	5.97	0.82	1	3	2
6.4	Lightspeed RT16	80	Variable	L	6.40	0.43	1	3	2

4.3.2 6.4 mm 120 kV Sphere Results

Table 9 summarizes the results for 4 mm spheres at 120 kV and different mA. The physicians' rating of the images taken from all the scanners at 120 kV, 35 mA, and a pitch greater than 1 showed little variation from machine to machine. Three of the physicians rated the image as acceptable for the Sensation 16. None of the physicians rated the sphere within the image as round. The average measurement of the sphere was 7.50 ± 0.71 mm. For the Sensation 64, two of the physicians rated the image as

acceptable. None of the physicians rated the sphere within the image as round. The average measurement for the Sensation 64 was 7.50 ± 0.50 mm. For the Lightspeed RT16, three of the physicians rated the image as acceptable. None of the physicians rated the image as round. The average measurement for the Lightspeed RT16 was 7.63 ± 0.97 mm.

The physicians' rating of the images taken from all the scanners at 120 kV, 35 mA, and a pitch less than 1 showed little variation from machine to machine. All of the physicians rated the image as acceptable for the Sensation 16. One of the physicians rated the sphere within the image as round. The average measurement of the sphere was 7.30 ± 1.25 mm. For the Sensation 64, three of the physicians rated the image as acceptable. One of the physicians rated the sphere within the image as round. The average measurement for the Sensation 64 was 6.67 ± 1.25 mm. For the Lightspeed RT16, three of the physicians rated the image as acceptable. Two of the physicians rated the image as round. The average measurement for the Lightspeed RT16 was 5.57 ± 1.23 mm.

The physicians' rating of the images taken from all the scanners at 120 kV, 50 mA, and a pitch greater than 1 showed little variation from machine to machine. All of the physicians rated the image as acceptable for the Sensation 16. Two of the physicians rated the sphere within the image as round. The average measurement of the sphere was 8.00 ± 1.22 mm. For the Sensation 64, all of the physicians rated the image as acceptable. Three of the physicians rated the sphere within the image as round. The average measurement for the Sensation 64 was 5.40 ± 0.42 mm. For the Lightspeed RT16, three of the physicians rated the image as acceptable. One of the physicians rated the image as round. The average measurement for the Lightspeed RT16 was 6.40 ± 0.43 mm.

The physicians' rating of the images taken from all the scanners at 120 kV, 50 mA, and a pitch less than 1 showed little variation from machine to machine. All of the physicians rated the image as acceptable for the Sensation 16. One of the physicians rated the sphere within the image as round. The average measurement of the sphere was 6.63 ± 0.96 mm. For the Sensation 64, all of the physicians rated the image as acceptable. Two of the physicians rated the sphere within the image as round. The average measurement for the Sensation 64 was 7.25 ± 1.03 mm. For the Lightspeed RT16, three of the physicians rated the image as acceptable. None of the physicians rated the image as round. The average measurement for the Lightspeed RT16 was 6.63 ± 0.45 mm.

The physicians' rating of the images taken from all the scanners at 120 kV, a variable current, and a pitch greater than 1 showed little variation from machine to machine. All of the physicians rated the image as acceptable for the Sensation 16. Two of the physicians rated the sphere within the image as round. The average measurement of the sphere was 6.68 ± 0.90 mm. For the Sensation 64, three of the physicians rated the image as acceptable. None of the physicians rated the sphere within the image as round. The average measurement for the Sensation 64 was 7.85 ± 1.25 mm. For the Lightspeed RT16, all of the physicians rated the image as acceptable. None of the physicians rated the image as round. The average measurement for the Lightspeed RT16 was 6.33 ± 0.47 mm.

The physicians' rating of the images taken from all the scanners at 120 kV, a variable current, and a pitch less than 1 showed little variation from machine to machine. All of the physicians rated the image as acceptable for the Sensation 16. None of the physicians rated the sphere within the image as round. The average measurement of the sphere was

7.48 ± 0.53 mm. For the Sensation 64, three of the physicians rated the image as acceptable. None of the physicians rated the sphere within the image as round. The average measurement for the Sensation 64 was 7.33 ± 0.94 mm. For the Lightspeed RT16, three of the physicians rated the image as acceptable. None of the physicians rated the image as round. The average measurement for the Lightspeed RT16 was 7.33 ± 0.84 mm.

Table 9: 6.4 mm 120 kV Sphere Results. Only acceptable images were judged for roundness and measured for sizes.

Sphere	Center	kV	mA	Pitch	Average	St. Dev.	Unacceptable	Acceptable	Round
6.4	Lightspeed RT16	120	35	H	7.63	0.97	1	3	0
6.4	Sensation 16	120	35	H	7.50	0.71	1	3	0
6.4	Sensation 64	120	35	H	7.50	0.50	2	2	0
6.4	Lightspeed RT16	120	35	L	5.57	1.23	1	3	2
6.4	Sensation 16	120	35	L	7.30	1.25	0	4	1
6.4	Sensation 64	120	35	L	6.67	1.25	1	3	1
6.4	Lightspeed RT16	120	50	H	6.40	0.43	1	3	1
6.4	Sensation 16	120	50	H	8.00	1.22	0	4	2
6.4	Sensation 64	120	50	H	5.40	0.42	0	4	3
6.4	Lightspeed RT16	120	50	L	6.63	0.45	1	3	0
6.4	Sensation 16	120	50	L	6.63	0.96	0	4	1
6.4	Sensation 64	120	50	L	7.25	1.03	0	4	2
6.4	Lightspeed RT16	120	Variable	H	7.85	1.25	0	4	0
6.4	Sensation 16	120	Variable	H	6.68	0.90	0	4	2
6.4	Sensation 64	120	Variable	H	6.33	0.47	1	3	0
6.4	Lightspeed RT16	120	Variable	L	7.13	0.84	1	3	0
6.4	Sensation 16	120	Variable	L	7.48	0.53	0	4	0
6.4	Sensation 64	120	Variable	L	7.33	0.94	1	3	0

4.4 8 mm Sphere Results

4.4.1 8 mm 80 kV Sphere Results

Table 10 summarizes the results for 4 mm spheres at 120 kV and different mA. The physicians' rating of the images taken from all scanners at 80 kV and 50 mA showed little variation from machine to machine. Three of the physicians rated the image as

acceptable for the Sensation 16. Three of the physicians rated the sphere within the image as round. The average measurement of the sphere was 6.33 ± 0.94 mm. For the Sensation 64, three of the physicians rated the image as acceptable. Three of the physicians rated the sphere within the image as round. The average measurement for the Sensation 64 was 8.67 ± 0.47 mm. For the Lightspeed RT16, two of the physicians rated the image as acceptable. One of the physicians rated the image as round. The average measurement for the Lightspeed RT16 was 6.90 ± 0.10 mm.

The physicians' rating of the images taken from all the scanners at 80 kV and 100 mA showed little variation from machine to machine. All of the physicians rated the image as acceptable for the Sensation 16. All of the physicians rated the sphere within the image as round. The average measurement of the sphere was 7.58 ± 0.63 mm. For the Sensation 64, three of the physicians rated the image as acceptable. Three of the physicians rated the sphere within the image as round. The average measurement for the Sensation 64 was 7.13 ± 1.03 mm.

The physicians' rating of the images taken from all the scanners at 80 kV and a variable current showed little variation from machine to machine. Three of the physicians rated the image as acceptable for the Sensation 16. Three of the physicians rated the sphere within the image as round. The average measurement of the sphere was 6.93 ± 0.90 mm. For the Sensation 64, three of the physicians rated the image as acceptable. Three of the physicians rated the sphere within the image as round. The average measurement for the Sensation 64 was 7.13 ± 1.03 mm. For the Lightspeed RT16, three of the physicians rated the image as acceptable. Three of the physicians rated the image as round. The average measurement for the Lightspeed RT16 was 8.10 ± 0.29 mm.

4.4.2 8 mm 120 kV Sphere Results

Table 11 summarizes the results for 4 mm spheres at 120 kV and different mA. The physicians' rating of the images taken from all scanners at 120 kV, 35 mA, and a pitch greater than 1 showed little variation from machine to machine. All of the physicians rated the image as acceptable for the Sensation 16. All of the physicians rated the sphere within the image as round. The average measurement of the sphere was 6.98 ± 0.04 mm. For the Sensation 64, all of the physicians rated the image as acceptable. All of the physicians rated the sphere within the image as round. The average measurement for the Sensation 64 was 7.60 ± 0.42 mm. For the Lightspeed RT16, three of the physicians rated the image as acceptable. Three of the physicians rated the image as round. The average measurement for the Lightspeed RT16 was 7.67 ± 0.47 mm.

Table 10: 8 mm 80 kV Sphere Results. Only acceptable images were judged for roundness and measured for sizes.

Sphere	Center	kV	mA	Pitch	Average	St. Dev.	Unacceptable	Acceptable	Round
8	Sensation 16	80	50	H	6.33	0.94	1	3	3
8	Sensation 64	80	50	H	8.67	0.47	1	3	3
8	Lightspeed RT16	80	50	L	6.90	0.10	2	2	1
8	Sensation 16	80	100	H	7.58	0.63	0	4	4
8	Sensation 64	80	100	H	7.13	1.03	1	3	3
8	Sensation 16	80	Variable	H	6.93	0.90	1	3	3
8	Sensation 64	80	Variable	H	7.13	1.03	1	3	3
8	Lightspeed RT16	80	Variable	L	8.10	0.29	1	3	3

The physicians' rating of the images taken from all scanners at 120 kV, 35 mA, and a pitch less than 1 showed little variation from machine to machine. All of the physicians rated the image as acceptable for the Sensation 16. All of the physicians rated the sphere within the image as round. The average measurement of the sphere was 7.58 ± 0.70 mm. For the Sensation 64, all of the physicians rated the image as acceptable. All of the physicians rated the sphere within the image as round. The average measurement for the

Sensation 64 was 6.70 ± 0.41 mm. For the Lightspeed RT16, three of the physicians rated the image as acceptable. Three of the physicians rated the image as round. The average measurement for the Lightspeed RT16 was 7.37 ± 0.45 mm.

The physicians' rating of the images taken from all scanners at 120 kV, 50 mA, and a pitch greater than 1 showed little variation from machine to machine. All of the physicians rated the image as acceptable for the Sensation 16. All of the physicians rated the sphere within the image as round. The average measurement of the sphere was 7.73 ± 0.53 mm. For the Sensation 64, all of the physicians rated the image as acceptable. All of the physicians rated the sphere within the image as round. The average measurement for the Sensation 64 was 7.83 ± 0.20 mm. For the Lightspeed RT16, three of the physicians rated the image as acceptable. Three of the physicians rated the image as round. The average measurement for the Lightspeed RT16 was 7.47 ± 0.41 mm.

The physicians' rating of the images taken from all scanners at 120 kV, 50 mA, and a pitch less than 1 showed little variation from machine to machine. All of the physicians rated the image as acceptable for the Sensation 16. All of the physicians rated the sphere within the image as round. The average measurement of the sphere was 7.90 ± 0.73 mm. For the Sensation 64, all of the physicians rated the image as acceptable. All of the physicians rated the sphere within the image as round. The average measurement for the Sensation 64 was 7.50 ± 0.50 mm. For the Lightspeed RT16, three of the physicians rated the image as acceptable. Three of the physicians rated the image as round. The average measurement for the Lightspeed RT16 was 7.60 ± 0.43 mm.

The physicians' rating of the images taken from all scanners at 120 kV, a variable current, and a pitch greater than 1 showed little variation from machine to machine. All

of the physicians rated the image as acceptable for the Sensation 16. All of the physicians rated the sphere within the image as round. The average measurement of the sphere was 7.50 ± 0.50 mm. For the Sensation 64, all of the physicians rated the image as acceptable. All of the physicians rated the sphere within the image as round. The average measurement for the Sensation 64 was 8.08 ± 0.13 mm. For the Lightspeed RT16, three of the physicians rated the image as acceptable. Three of the physicians rated the image as round. The average measurement for the Lightspeed RT16 was 7.40 ± 0.64 mm.

Table 11: 8 mm 120 kV Sphere Results. Only acceptable images were judged for roundness and measured for sizes.

Sphere	Center	kV	mA	Pitch	Average	St. Dev.	Unacceptable	Acceptable	Round
8	Lightspeed RT16	120	35	H	7.67	0.47	1	3	3
8	Sensation 16	120	35	H	6.98	0.04	0	4	4
8	Sensation 64	120	35	H	7.60	0.42	0	4	4
8	Lightspeed RT16	120	35	L	7.37	0.45	1	3	3
8	Sensation 16	120	35	L	7.58	0.70	0	4	4
8	Sensation 64	120	35	L	6.70	0.41	0	4	4
8	Lightspeed RT16	120	50	H	7.47	0.41	1	3	3
8	Sensation 16	120	50	H	7.73	0.53	0	4	4
8	Sensation 64	120	50	H	7.83	0.20	0	4	4
8	Lightspeed RT16	120	50	L	7.60	0.43	1	3	3
8	Sensation 16	120	50	L	7.90	0.73	0	4	4
8	Sensation 64	120	50	L	7.50	0.50	0	4	4
8	Lightspeed RT16	120	Variable	H	7.40	0.64	1	3	3
8	Sensation 16	120	Variable	H	7.50	0.50	0	4	4
8	Sensation 64	120	Variable	H	8.08	0.13	0	4	4
8	Lightspeed RT16	120	Variable	L	7.40	0.42	0	4	4
8	Sensation 16	120	Variable	L	7.20	0.79	0	4	4
8	Sensation 64	120	Variable	L	7.90	0.50	0	4	4

The physicians' rating of the images taken from all scanners at 120 kV, a variable current, and a pitch less than 1 showed little variation from machine to machine. All of the physicians rated the image as acceptable for the Sensation 16. All of the physicians rated the sphere within the image as round. The average measurement of the sphere was

7.20 ± 0.79 mm. For the Sensation 64, all of the physicians rated the image as acceptable. All of the physicians rated the sphere within the image as round. The average measurement for the Sensation 64 was 7.90 ± 0.50 mm. For the Lightspeed RT16, all of the physicians rated the image as acceptable. All of the physicians rated the image as round. The average measurement for the Lightspeed RT16 was 7.40 ± 0.42 mm.

4.5 Summary of Sphere Results

For all the spheres, the Lightspeed RT16 had the most images rated as unacceptable and the Sensation 16 had the least images rated as unacceptable. The Lightspeed RT16 overestimated the size of the sphere more often than the other two scanners. For all the spheres, 120 kV had the most images rated as acceptable. Using 80 kV caused physicians to overestimate the size of the sphere more often than using 120 kV. The larger sphere size had the most images rated as acceptable; almost all of these images were rated as acceptable. The smaller sphere sizes caused physicians to overestimate the size of the sphere more than the larger spheres. For all the spheres, a larger current had the most images rated as acceptable. Within individual sphere size, if an image was rated as acceptable, the current did not affect the amount of image sizes overestimated.

4.6 CTDI Results

The CTDI measurements differed from the acquisition software for each of the parameter settings. The CTDI comparisons are shown in **Table 12**, organized by the acquisition parameters. The measured CTDI was lower than the CTDI reported by the acquisition software foremost of acquisition parameters. The CTDI calculated for the Lightspeed RT16 differed by a minimum of 16.90%. This scanner by far showed the most deviation from the estimated CTDI. Although these measurements were very

different from the estimate, in each case the measured CTDI was lower than the CTDI reported by the scanner so it is reasonable to base the “low-dose acquisition parameters” on the scanner reported values. The CTDI calculated for the Sensation 16 differed by a maximum of -10.35%. The CTDI calculated for the Sensation 64 differed by a maximum of -4.46%. This scanner showed the least deviation from the estimated CTDI. In most cases, the CTDIs for 80 kV differed more than the CTDIs for 120 kV. In 4 of 6 cases, the scanner estimates less reliable for the lower mA setting. One reason the Lightspeed RT16 was so much worse than the other two scanners is the Lightspeed RT16 is primarily used for treatment planning whereas the other two are used for diagnosis. In the case of treatment planning, the dose received from a CT scan is so much lower than the dose a patient is being treated to that it would not be as important.

Table 12: CTDI Comparison: Organized by Scanner and Acquisition Parameters

Machine	Energy(kV)	Current (mA)	Rotation Speed	# of detector rows	Slice thickness	Reported CTDI (mGy)	Measured CTDI (mGy)	p	% Diff
Lightspeed RT16	80	50	0.8	16	1.25	0.96	0.75±0.016	0.0002	21.60%
Lightspeed RT16	80	100	0.8	16	1.25	1.92	1.52±0.027	0.0001	21.09%
Lightspeed RT16	120	35	0.8	16	1.25	2.05	1.67±0.030	0.0002	18.50%
Lightspeed RT16	120	50	0.8	16	1.25	2.93	2.37±0.048	0.0003	19.22%
Lightspeed RT16	120	100	0.8	16	1.25	5.86	4.87±0.155	0.0032	16.90%
Sensation 16	80	50	0.75	12	1.5	1.16	1.28±0.007	0.00009	-10.35%
Sensation 16	80	100	0.75	12	1.5	2.31	2.39±0.068	0.1989	-3.40%
Sensation 16	120	35	0.75	12	1.5	2.54	2.49±0.035	0.1480	2.03%
Sensation 16	120	50	0.75	12	1.5	3.62	3.30±0.057	0.0052	8.78%
Sensation 16	120	100	0.75	12	1.5	7.24	6.64±1.45	0.1389	8.27%
Sensation 64	80	50	0.5	24	1.2	0.9	0.88±0.001	0.00001	2.33%
Sensation 64	80	100	0.5	24	1.2	1.8	1.73±0.012	0.4411	3.91%
Sensation 64	120	35	0.5	24	1.2	2.36	2.47±0.004	0.00001	-4.46%
Sensation 64	120	50	0.5	24	1.2	3.37	3.28±0.070	0.1671	2.80%
Sensation 64	120	100	0.5	24	1.2	6.74	6.65±0.009	0.0006	1.26%

CHAPTER 5: CONCLUSION

Our study showed that physicians were reasonably able to judge the size and shape of nodules accurately using low-dose CT. The advantages of this can be taken over to screening for lung nodules.

The investigation was performed for two tube voltages, three machines, and several currents. A CTDI dose of 1.5 mGy was used as a target dose for this study. Of the two voltages, 80 kV was shown to be an ineffective voltage to because 80 kV images were consistently rated as unacceptable quality, hindering the physicians' ability to determine nodule size. Between the three machines, there was not a substantial difference in perceived image quality or consistency of physicians' measurements when a current of 50 mA or higher was used. 50 mA showed an image quality that was acceptable and physicians were able to determine the size of the nodules as well as when a 100 mA or variable current was used. These parameters are acceptable, 120 kV, 50 mA, 120 mA, and pitch between 0.94 and 1.4. These parameters are not acceptable, 80 kV and 35 mA. Here is the protocol we recommend: 120 kV, 50 mA, and a 1.4 pitch. This will produce a CTDI between 2.13-3.83 mGy. From the acquisition parameters recommended, a CTDI dose of 1.5 mGy could not be met. From the three scanners evaluated, it appears that the CTDI estimated by the scanner consistently overestimated the delivered CTDI, for the recommended parameters.

We found our hypothesis to be incorrect. We found that the acquisition parameters used affected the physicians' ability to judge size and shape of a lung nodule in low dose CT more than dose level. Even though a scan at a lower kV with a higher mA can produce a similar CTDI to a scan at a higher kV with a lower mA, the physicians

consistently indicated that the lower kV images were less likely to be acceptable. A reduction in kV to achieve lower dose particularly seems to be a poor choice in terms of maintaining image quality. Furthermore, we found that the sphere size influence the physicians' assessment of acceptable image quality, with small sphere requiring the use of higher-dose acquisition parameters. This indicates that attempts at dose reduction by changing acquisition parameters should not be made arbitrarily, but rather should be carefully investigated in terms of task-based performance.

In future work, consideration must be given to the fact that lung nodules may exhibit a range of possible densities. This study used only acrylic spheres to keep the number of images to a manageable number for the physicians to assess and to eliminate detectability as a variable. Equivalent studies should be done with other sphere materials. There are also several acquisition parameters that were not considered for this study. In addition, the lung phantom used was a phantom intended for use with nuclear medicine. In the future, a study should be done using a phantom designed specifically for CT imaging. Finally, the task-based physician assessment should include a large number of images to allow a more substantial statistical assessment.

REFERENCES

- Aberle, D.R. (2001). A Consensus Statement of the Society of Thoracic Radiology Screening for Lung Cancer with Helical Computed Tomography. *Journal of Thoracic Imaging*, 16, 65-68.
- Archer, B. R., Gray, J. E., Dixon, R. L. and et al. (2004). NCRP Report 147 Structural Shielding Design for Medical X-Ray Imaging Facilities: National Council on Radiation Protection and Measurements.
- Bach, Peter B. (2012). Benefits and Harms of CT Screening for Lung Cancer. *The Journal of the American Medical Association*, 307(22), 2418-2429.
- Brenner, David J. (2004). Radiation Risks Potentially Associated with Low-Dose CT Screening of Adult Smokers for Lung Cancer. *Radiology*, 231, 440-445.
- Bushberg, Seibert, Leidholdt, Boone (2002). "The Essential Physics of Medical Imaging, Second Edition", Philadelphia, PA, Lippincott Williams & Wilkins.
- Cody, Dianna D. (2010). Normalized CT Dose Index of the CT Scanners Used in the National Lung Screening Trial. *American Journal of Roentgenology*, 194(6), 1539-1546.
- Fawcett, Tom. (2006). An Introduction to ROC analysis. *Pattern Recognition Letters*, 27, 861-874.
- Hasegawa, M. (2000). Growth Rate of Small Lung Cancers Detected on Mass CT Screening. *The British Journal of Radiology*, 73, 1252-1259.
- Henschke, Claudia I. (2004). CT Screening for Lung Cancer: Suspiciousness of Nodules according to Size on Baseline Scans. *Radiology*, 231, 164-168.
- Heuvers, Marlies E. (2012). Improving Lung Cancer Survival; Time to Move on. *BioMed Central*, 12(77), 1-4.
- Kalra, Mannudeep K. (2004). Strategies for CT Radiation Dose Optimization. *Radiology*, 230, 619-628.
- MacMahon, Heber. (2005). Guidelines for Management of Small Pulmonary Nodules Detected on CT Scans: A Statement from the Fleischner Society. *Radiology*, 237, 395-400.
- Mayo, John R. (2003). Radiation Exposure at Chest CT: A Statement of the Fleischner Society. *Radiology*, 228, 15-21.

Mazzone, Peter. (2012). The Rationale for, and Design of, a Lung Cancer Screening Program. *Cleveland Clinic Journal of Medicine*, 79(5), 337-345.

McCollough, Cynthia, Cody, D., Edyvean, S. and et al. (2008). The Measurement, Reporting, and Management of Radiation Dose in CT. College Park, MD: American Association of Physicists in Medicine.

Oguchi, K. (2000). Optimal Tube Current for Lung Cancer Screening with Low-Dose Spiral CT. *Acta Radiologica*, 41, 352-356.

Paul, N. S. (2007). Investigating the Low-Dose Limits of Multidetector CT in Lung Nodule Surveillance. *Medical Physics*, 34(9), 3587-3595.

Revel, Marie-Pierre. (2004). Are two-dimensional CT Measurements of Small Noncalcified Pulmonary Nodules Reliable? *Radiology*, 231, 453-458.

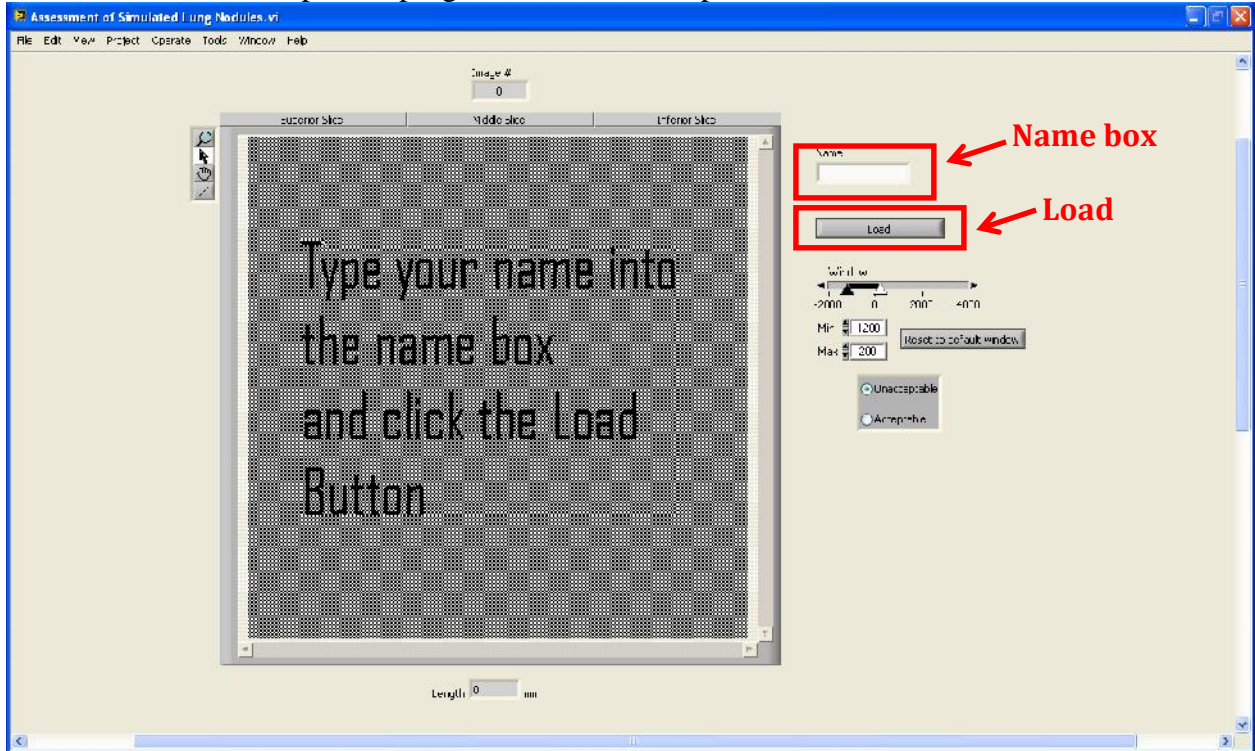
Sobue, Tomotaka. (2002). Screening for Lung Cancer with Low-Dose Helical Computed Tomography: Anti-Lung Cancer Association Project. *American Society of Clinical Oncology*, 20, 911-920.

Taiwo, Evelyn O. (2012). How Have We Diagnosed Early-Stage Lung Cancer without Radiographic Screening? A Contemporary Single-Center Experience. *PLoS ONE*, 7(12).

U.S. Cancer Statistics Working Group. *United States Cancer Statistics: 1999-2009 Incidence and Mortality Web-based Report* Atlanta, GA: Department of Health and Human Services, Centers for Disease Control and Prevention, and National Cancer Institute; 2013.

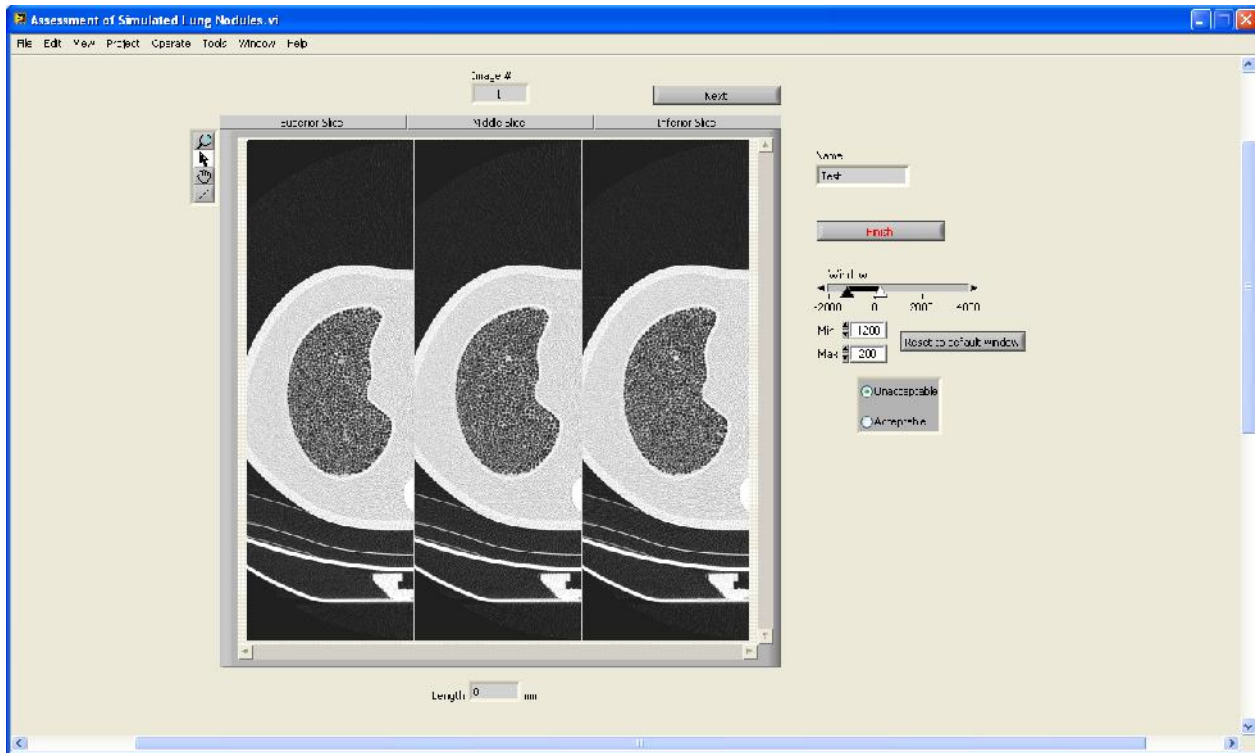
APPENDIX: PHYSICIAN INSTRUCTIONS

To begin, double-click the icon labeled “Assessment of Simulated Lung Nodules” which is located on the desktop. The program window will open and looks like this:

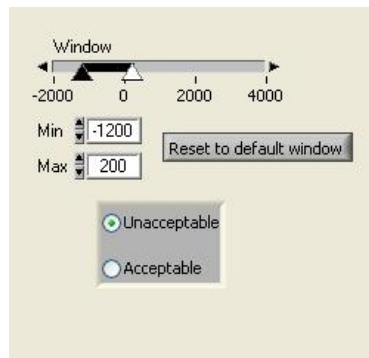


1. Type your name in the Name box, and click the “Load” button.
 - a. If you exit the program and wish to start where you left off, enter the same name into the Name box. If you wish to restart completely, enter a new name.

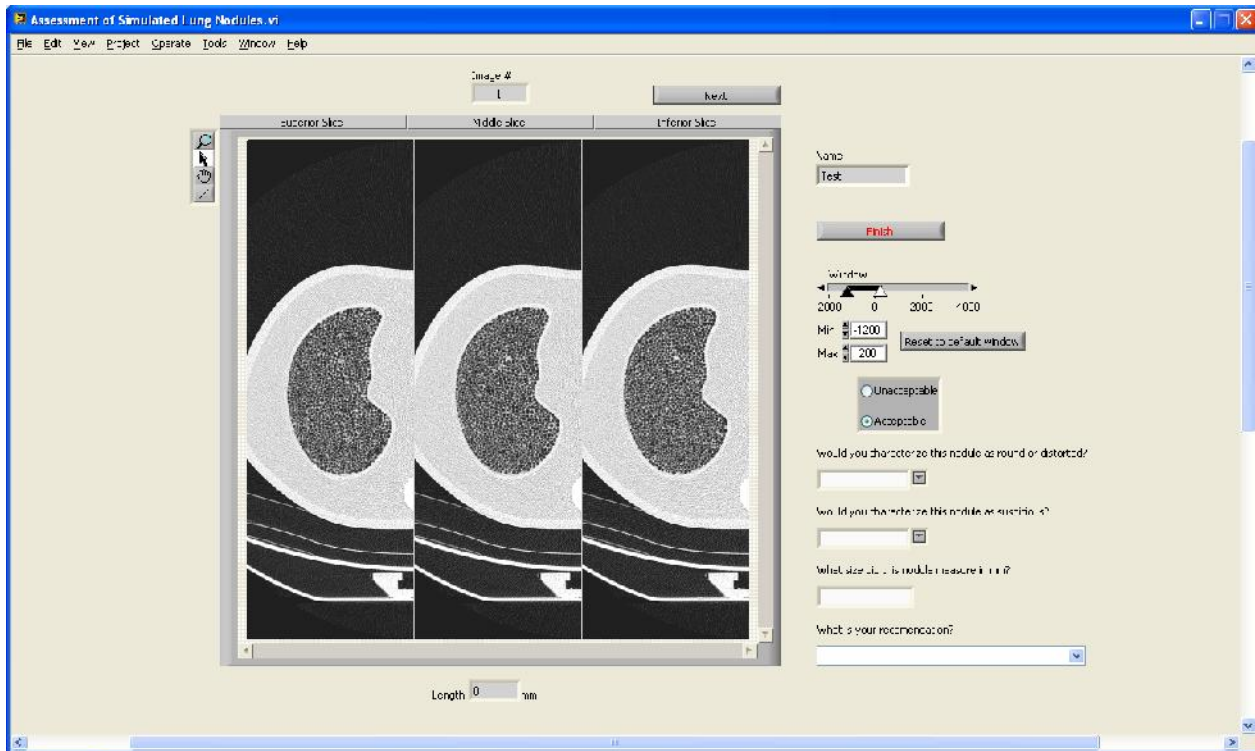
2. The first image will be brought up. The program window will look like this:



Adjust the window and level using the slider bars or by entering numbers into the boxes (Reset the window and level to the default value using the Reset to default window button)



Decide whether the image quality is acceptable or not and click the radio button corresponding to that decision (if unacceptable click next at this point)



If the image is acceptable 4 boxes will appear below the radio buttons.
 Looking at the nodule determine if you consider it round or distorted and select from the drop down box
 Next measure the nodule length using the line tool and whichever slice you deem appropriate (it may be helpful to zoom in using the zoom tool) (the only way to zoom out is to hold shift and use the zoom tool)
 If the nodule is distorted, measure the long axis dimension.



← Zoom Tool

← Pan Tool

← Line Tool

Enter this number into the appropriate box
 Next select a recommended course of action for this particular nodule
 Now click the next button to move to the next image
 Repeat the steps until all images are complete
 Click Finish at any point to save your progress or complete the program

VITA

Kendrick Williams was born in Plaquemine, Louisiana in October 1989. He is the son of Kendrick Williams and Andra Taplin. Kendrick is married to Jillana Williams. Kendrick received his Bachelors of Science Degree in Physics from Xavier University of Louisiana in May 2010. Upon completion of his degree, Kendrick enrolled at Louisiana State University to study Medical Physics. His future plans are to attend medical school.